THERMAL CONDUCTIVITY OF $CuK_2Cl_4 \cdot 2H_2O$ IN APPLIED MAGNETIC FIELDS NEAR ITS CURIE POINT

By

ROBERT WENDELL JOHNSON

Bachelor of Science in Electrical Engineering
University of Kansas
Lawrence, Kansas
1948

Master of Science
University of Kansas
Lawrence, Kansas
1952

Submitted to the Faculty of the Graduate College
of the Oklahoma State University
in partial fulfillment of the requirements
for the Degree
DOCTOR OF PHILOSOPHY
July 26, 1974

THERMAL CONDUCTIVITY OF $CuK_2Cl_4 \cdot 2H_2O$ IN APPLIED MAGNETIC FIELDS NEAR ITS CURIE POINT

Thesis Approved:

George S. Darby
Thesis Adviser

Jack J. Martin

James Lange

T. M. Wilson

James R. Clarke

D. D. Durham
Dean of the Graduate College

ACKNOWLEDGEMENTS

I wish to thank Dr. George Dixon for his patient endurance during my efforts to learn. Thanks is due also to Dr. Martin for advice and help in the operation of cryogenic equipment. I acknowledge the committee, who have inspired me to be creative. I am grateful for a summer fellowship in 1971 from the Research Corporation, and for summer support in 1972 from the National Science Foundation. But I owe my greatest thanks to my wife, Karen, who was willing to put up with many problems occasioned by this effort, and my children, David and Mark, who tolerated my preoccupation with reluctance.

TABLE OF CONTENTS

LIST OF TABLES

LIST OF FIGURES

LIST OF SYMBOLS

K_H - Thermal conductivity, K(H, T)

K_D - Saturated thermal conductivity; $H >> K_B T/g\beta$

G(H, T) - Thermal average $\langle \tau_M^{-1} \tau_D \rangle$ in terms of K_D, K_H :

$$G(H, T) = \frac{K_D - K_H}{K_H}$$

G_c - The critical isotherm $G(H, T_c)$

Λ - The relative isotherms $G(H, T)/G(H, T_c)$

Ω, Ω' - Magnetic relaxation rates of order parameter fluctuations

Λ_o - The value of Λ when $\Omega' = 0$, according to the model

Z - The regime index $\frac{\Omega}{XT} = \frac{\Omega'}{\omega}$

$\lambda(H, T)$ - The critical exponent describing critical behavior of Ω'

C_H - Specific heat at constant H

α_o - Hypothetical small negative critical exponent for specific heat at H = 0

α - The hypothetical field-dependent critical exponent for specific heat

z - Critical index for relaxation rate for order parameter fluctuations

CHAPTER I

INTRODUCTION

A. Thesis Objective

This dissertation reports low temperature measurements of thermal conductivity for the insulating ferromagnet $CuK_2Cl_4 \cdot 2H_2O$. These measurements are applied through the Debye theory of thermal conductivity to an investigation of phonon scattering due to magnetic ordering in applied magnetic fields, through the critical temperature of the magnetic phase transition. The temperature range of the study is $.6 < T < 1.5$ K, with most of the data below 1 K.

A reason for selection of cupri halides for study in general is that such crystals have Curie points[1] of the order of 1 K, at which temperatures the non-magnetic background scattering is relatively low, and the simple Debye-Callaway Theory[2] is appropos.

Another reason for the selection is the belief that next nearest-neighbor exchange is important in the interactions, and that these are closely approximated by the isotropic Heisenberg model.[3] Such crystals have a body-centered tetragonal structure, with low distortion from cubic symmetry.

Magnetic phonon scattering is studied along isotherms as a function of applied magnetic field, and along isochamps as a function of temperature for low fields. Previous studies[4] on this material have shown that the zero field conductivity in the paramagnetic phase can be

accounted for by scattering of phonons from magnetic critical fluctuations. The basis for the relaxation rate describing this scattering is discussed in the theory section. An attempt is made to account for the low-field temperature dependence using a similar relaxation rate. The behavior of the relaxation rate as a function of applied field is obtained and compared with simple model calculations.

B. Critical Phenomena

Whenever any two of three thermodynamic variables, connected by an equation of state for a substance are plotted in a plane, there appear regions separated by boundaries: This is a phase diagram. The regions each represent either one phase, or two phases coexisting. In such plots, one boundary has a point associated with a certain temperature, T_c, at which phases adjacent to this boundary become physically indistinguishable. This is the critical point, labelled by T_c. The behavior of thermodynamic variables near the critical point is called critical phenomena; subsequent discussion is concerned with magnetic phase transitions near T_c, where T_c is the limiting temperature at and above which they can occur.

1. Critical Exponents

A most fascinating discovery, about which most has been learned in the past ten years, is that the behavior of properties near phase transitions can be described by laws involving small-number exponents.

A critical exponent is defined as follows. Let

$$\epsilon = \frac{\Delta T}{T_c} = \frac{T - T_c}{T_c}$$

be a dimensionless independent variable. Let a general property of the

system be described by the function f (ϵ), the behavior of which is to be studied near the critical temperature, T_c. It is assumed f (ϵ) is continuous for $\epsilon \neq 0$. Then

$$\lim_{\epsilon \to \pm 0} \frac{\ln f(\epsilon)}{\ln \epsilon} = \lambda$$

is called the critical exponent associated with the function f (ϵ), and is assumed to exist.

It is necessary to distinguish in some cases the approach from below T_c, $\epsilon \to -0$, from the approach from above T_c, $\epsilon \to +0$, because the exponents may be different.

An important example is the exponent β, characteristic of order parameters. A typical order parameter is the magnetization for a ferromagnet. An order paramenter, p, is so called because it is non vanishing only in the ordered phase. The relation

$$\langle p \rangle = a|\epsilon|^{p}$$

is found valid near T_c, where a is a constant. Experimentally, the value of β appears to be very near the fraction 1/3 for some widely desparate systems, but there is a growing list of materials for which deviations from the value 1/3 are significant.

Examples illustrating the general application of certain exponents for analogous properties abound; a good reference is the monograph by Stanley.[5]

This discussion is to be confined to magnetic phase transitions; analogous behavior in fluid and other systems is referenced. The critical points for ferromagnetic and antiferromagnetic phenomena are respectively the Curie point T_c, and the Neil point, T_n. Beneath T_c there is spontaneous magnetization, above T_c an external field is required to induce magnetization. The magnetization from below is accurately repre-

sented by[5]

$$M = M_m |\epsilon|^{\beta}$$

under zero field, where M is the order parameter and M_m is constant. M vanishes as $\epsilon \rightarrow 0$.

2. Fluctuations in the Order Parameter

L. Onsager[6] found in 1944 the partition function for the Ising model of crystal magnetization in two dimensions for zero field. He then derived thermodynamic properties. His finding that the specific heat had a logarithmic singularity at the critical point suggested that the finite discontinuities in the derivatives of thermodynamic potentials at the critical point, according to Ehrenfest's scheme,[7] might instead be singularities for real substances in some cases. This suggestion was later supported in 1958 by Buckingham, Fairbank, and Kellers,[8] in an experiment with ^{4}He: Specific heat was found to be divergent to within a micro degree of the λ-point. It is now believed that at least some second order derivatives of the Gibbs and Helmholtz potentials are divergent at the critical point. The source of singularities in the thermodynamic derivatives near the critical point is large scale fluctuations in the order parameter.

Basically, a fluctuation is a deviation of a function describing a property from the ensemble average for this function. Interest here is in steady-state, or time-independent fluctuations, which depend in general upon position, $\vec{r}$.

Thus, the fluctuation at position $\vec{r}_1$ for an order parameter $p(\vec{r}_1)$ is $\delta p_1 = p(\vec{r}_1) - p_o(\vec{r}_1)$, where p_o is the ensemble average at $\vec{r}_1$. Considering another fluctuation, δp_2 at $\vec{r}_2$, one finds convenient

the definition of the joint fluctuation, $\delta p_1 \, \delta p_2$, in arriving at the pair-correlation function:

$$g(\vec{r}_1, \vec{r}_2) = \int_V \int_V \delta p_1 \; \delta p_2 \; dV_1 \; dV_2 .$$

This double-volume integral affords analytical treatment of fluctuations. The case that $g = 0$ implies that deviations are independent at the different positions, $\vec{r}_1$ and $\vec{r}_2$. The function measures a conditional probability: that of finding a value of p in the neighborhood of $\vec{r}_2$ if this value were found near $\vec{r}_1$.

Ornstein and Zernike[9] derived the pair correlation function in 1914; it is modified to date by introducing a small critical exponent, n:

$$g(r) = \frac{e^{-r/\xi}}{r^{d-2+n}}$$

It is semi-empirical, and applicable to d = 3, 2, or 1 dimension models. Here $r = |\vec{r}_1 - \vec{r}_2|$, and ξ is the temperature-dependent correlation length.

As one lowers temperature toward T_c, in the case of the magnetic phase transition, small islands of correlated moments begin to appear and grow in radius. The lifetime of these islands is also small, and grows as $T \to T_c$. An island has an ordered pattern; in the ferromagnetic case the moments are all parallel, in the anti-ferromagnetic case moments alternate consecutively in direction. The mean radius of an island is roughly the "correlation length," ξ. Above T_c there may be small islands of correlation, but the magnetizations of different islands are randomly oriented. Such order is said to be short-ranged. Below T_c there is a long-range order, the case of spontaneous magnetization. At T_c the radius and lifetime of these islands apply to the

magnetic domains of the ordered phase.

An intuitive picture of the effect of the magnetic phase transition on thermal conductivity emerges. Near the critical point, phonons are scattered by islands of correlated spin, of average radius ξ, analogous to the critical-opalescence phenomenon for light. This scattering increases the thermal resistance at the transition temperature.

3. Static Scaling Laws

No theory yet exists which connects the variety of exponents and the exponent laws observed empirically to hold near the critical point. However, a fruitful assumption that has had a unifying effect is the static scaling hypothesis. It simply supposes that the thermodynamic derivatives are characterized by a single ξ-parameter or correlation length. Then, specifically[10,11] a correlation function representative of any thermodynamic quantity is assumed to be a homogeneous function of r/ξ, or else of $q\xi$, where q is the wave-vector magnitude, $2\pi/\lambda$, for excitations of wave-length λ.* (A function $f(x,y,z,--)$ is homogeneous of degree n if, for any number t, $f(tx,ty,tz,--) = t^n f(x,y,z,--)$).

An earlier statement of the static scaling hypothesis is equivalent:[5] The Gibbs potential $G(\epsilon, H)$ is a generalized homogeneous function, which means that it is of such form that for any number, t,

---

*Kadanoff correlation-function scaling laws may possibly conflict with some calculations (see Stanley)[5].

$$G\left(t^{a_\epsilon}\epsilon,\ t^{a_H}H\right) = t\,G\left(H\epsilon,\ H\right)^{*} \qquad (1)$$

Here, a_H and a_ϵ are two exponents, or scaling parameters. If the hypothesis is valid it would follow that the other thermodynamic potentials, such as the Helmholtz, the enthalpy, and the internal energy, are also generalized homogeneous functions (see the reference).

The physical significance of such functions is that scaled relationships are possible. The generalized homogeneous properties can be used to express the independent variables as functions of one variable, (the correlation length), which sets the expanded scale to which the ordinates of one curve section are a simple multiple of the corresponding ordinates of another curve section. A set of plots such as $G(\epsilon, H)$ can be transformed via the proper scale ξ to one curve. One scales G in $\xi(\epsilon)$ dependent units: $\frac{G}{\mu(\xi)}$, and H similarly: $\frac{H}{w(\xi)}$, whence $\frac{G}{\mu(\xi)} = r\frac{H}{w(\xi)}$ is the scaled relation: $\mu(\xi)$ and $w(\xi)$ are scaling functions, r is a constant.

a. Relationships Among Critical Exponents

By thermodynamic considerations, stability criteria, and analysis of the geometric behavior of potential plots, a number of inequalities have been found connecting various critical exponents. A couple of these are here summarized.

Rushbrooke Inequality: for $H = 0$, $T \to T_c$, $\alpha' + 2\beta + r' \geq 2$

---

*A generalized homogeneous function G, of degree n, is defined by the condition $G\left(q^{m_1}x,\ q^{m_2}y,\ q^{m_3}z,\text{---}\right) = q^{n}G\left(x, y, z\text{---}\right)$ where q is any number, and m_1, m_2, ... are exponents. Let $q = t^{1/n}$, and the equivalent definition follows.

Griffith's Inequality: if $\left.\frac{\partial S}{\partial M}\right]_T \leq 0$ for $M \geq 0$, $T = T_c$, $\alpha' + \beta(\delta + 1) \geq 2$.

In Stanley's book can be found extensive tables of exponent inequalities.[5]

An important consequence of the scaling hypothesis is that the exponent inequalities become equalities. Experiments contradict the scaling relation $\alpha = \alpha'$, but otherwise as yet haven't distinguished equalities from inequalities.

For example, $\alpha' = 0$, $\beta = 1/8$, and $\gamma = 1\ 3/4$ apply to the two dimensional Ising model. These values satisfy the Rushbrooke expression as an equality. One may try other exponent values from appended Table I in the various inequalities: The result in each case is an equality, relating the exponents.

All of the various relations among the exponents are derivable under the static scaling assumption; it implies all of the critical exponents can be expressed in terms of only two scaling parameters a_H and a_ϵ : If any two critical exponents are known, the others can all be found.

The manner of finding critical exponent relationships is illustrated by example.[5] Differentiate (1) with respect to H, getting

$$t^{a_H} \frac{\partial G(t^{a_\epsilon}\epsilon, t^{a_H}H)}{\partial (t^{a_H}H)} = t \frac{\partial G(\epsilon, H)}{\partial H},$$

or (2)

$$t^{a_H} M(t^{a_\epsilon}\epsilon, t^{a_H}H) = t\, M(\epsilon, H).$$

If $H = 0$, $M(\epsilon, 0) = t^{a_H - 1} M(t^{a_\epsilon}\epsilon, 0)$; this holds for all t; take

$$t = (-\epsilon)^{-\frac{1}{a_\epsilon}}.$$

TABLE I

EXPONENT DEFINITIONS AND VALUES

Exponent	Definitions and experimental data		Exact and approximate theoretical values					Exponent
	$\Delta T = \lvert T - T_c \rvert$ Gas–liquid	Ferromagnet	Classical theory	Ising ($d = 2$)	Ising ($d = 3$)	Heisenberg ($d = 3$) ($S = \infty$)	Heisenberg ($d = 3$) ($S = \frac{1}{2}$)	
below T_c	at coexistence $T \to T_c-$	$H = 0, T \to T_c-$						*below* T_c
α'	$C_V \sim \Delta T^{-\alpha' \simeq 0(\log)}$	$C_H \sim \Delta T^{-\alpha' \simeq 0(\log)}$	0 (discon.)	0 (log)	$\frac{1}{16}{}^{+0.16}_{-0.035}$			α'
β	$\rho_L - \rho_G \sim \Delta T^{\beta \simeq 0.34}$	$M_0(T) \sim \Delta T^{\beta \simeq 0.33}$	$\frac{1}{2}$	$\frac{1}{8}$	$\frac{5}{16}{}^{+0.003}_{-0.006}$			β
γ'	$K_T \sim \Delta T^{-\gamma' \gtrsim 1.2}$	$\chi_T \sim \Delta T^{-\gamma'}$	1	$1\frac{3}{4}$	$1\frac{5}{16}{}^{+0.03}_{-0.05}$			γ'
ν'	$\kappa(T) \sim \Delta T^{\nu'}$	$\kappa(T) \sim \Delta T^{\nu'}$	$\frac{1}{2}$	1	$(0.675^{+0.02}_{-0.03})$			ν'
Δ'	$\partial^3 p/\partial \mu^3 \sim \partial K_T/\partial p \sim \Delta T^{-\gamma'-\Delta'}$ ⋮	$\partial^3 F/\partial H^3 \sim \Delta T^{-\gamma'-\Delta'}$ ⋮	$1\frac{1}{2}$	$1\frac{7}{8}$				Δ'
at $T = T_c$	$\rho \to \rho_c$	$M \to 0$						*at* $T = T_c$
δ	$\lvert p - p_c \rvert \sim \lvert \rho - \rho_c \rvert^{\delta \simeq 4.2}$	$\lvert H \rvert \sim \lvert M \rvert^{\delta \gtrsim 4.2}$	3	15	$5\frac{1}{2} \pm 0.15$			δ
η	$I_c(\mathbf{k})/I_0(\mathbf{k}) \sim 1/k^{2-\eta}$	$\hat{\chi}_c(\mathbf{k}) \sim 1/k^{2-\eta}$	0	$\frac{1}{4}$	$\frac{1}{16} \pm 0.008$	0.075 ± 0.035	$\simeq 0.08$	η
	$G_c(\mathbf{r}) \sim r^{-(d-2+\eta)} \quad \eta \gtrsim 0$	$\langle S_0{}^z S_{\mathbf{r}}{}^z \rangle \sim r^{-(d-2+\eta)} \quad \eta \gtrsim 0$						
above T_c	$\rho = \rho_c, T \to T_c+$	$H = 0, T \to T_c+$						*above* T_c
α	$C_V \sim \Delta T^{-\alpha \gtrsim 0}$	$C_H \sim \Delta T^{\alpha \simeq 0}$	0 (discon.)	0 (log)	$\frac{1}{8} \pm 0.015$	$\simeq 0$ (?)	$\simeq 0$ (?)	α
γ	$K_T \sim \Delta T^{-\gamma \gtrsim 1.2}$	$\chi_T \sim \Delta T^{-\gamma \simeq 1.35}$	1	$1\frac{3}{4}$	$1\frac{1}{4} \pm 0.003$	1.33 ± 0.01	1.43 ± 0.04	γ
ν	$\kappa(T) \sim \Delta T^{-\nu \gtrsim 0.6}$	$\kappa(T) \sim \Delta T^{-\nu \gtrsim 0.66}$	$\frac{1}{2}$	1	$\frac{9}{14} \pm 0.0025$	0.692 ± 0.012	$\simeq 0.74$	ν
Δ	—	$\partial^4 F/\partial H^4 \sim \Delta T^{-\gamma-2\Delta}$	$1\frac{1}{2}$	$1\frac{7}{8}$	$1\frac{9}{16} \pm 0.03$		1.81 ± 0.05	Δ

Source: M. E. Fisher, "Theory of Equilibrium Critical Phenomena," Reports on Progress in Physics, Part II, (1967).

Then,

$$M(\epsilon, 0) = (-\epsilon)^{\frac{1 - a_H}{a_\epsilon}} M(-1, 0).$$

But β is defined by an exponent law: $M(\epsilon, 0) \sim (-\epsilon)^{\beta}$, as $\epsilon \to 0^-$, whence,

$$\beta = \frac{1 - a_H}{a_\epsilon} . \tag{3}$$

Other detailed derivations after this fashion can be followed in Stanley's book.[5]

b. The Form of the Equation of State

Equation (2) is one example of an equation of state, relating variables M, H, and T. It can be put into the form

$$M(\epsilon, H) = t^{\frac{a_H - 1}{a_\epsilon}} M(t^{a_\epsilon}\epsilon, t^{a_H} H) .$$

Take

$$t = |\epsilon|^{-\frac{1}{a_\epsilon}}$$

whence,

$$M(\epsilon, H) = |\epsilon|^{\frac{1 - a_H}{a_\epsilon}} M\left(\frac{\epsilon}{|\epsilon|}, \frac{H}{|\epsilon|^{a_H/a_\epsilon}}\right) .$$

Using Equation (3), and another critical exponent relationship, $\frac{a_H}{a_\epsilon} = \Delta = \beta\delta$, one gets

$$m = \frac{M(\epsilon, H)}{|\epsilon|^{\beta}} = M\left(\frac{\epsilon}{|\epsilon|}, \frac{H}{|\epsilon|^{\beta\delta}}\right) = M(\pm 1, h),$$

where

$$h = \frac{H(\epsilon, M)}{|\epsilon|^{\beta\delta}}$$

is a scaled magnetic field and m the scaled magnetization. Plots of m versus h should be the same for all temperatures. This is borne out

in a plot from both supercritical ($T > T_c$) and subcritical ($T < T_c$) isotherm data in the insulating ferromagnet $CrBr_3$:Ho and Lister (1969).

C. Interaction of Phonons with Critical Fluctuations

1. Magnetic Relaxation Rate from Ultrasonic Attenuation

Calculations of phonon relaxation time for magnetic critical scattering have been based to date on theories that apply at low frequencies and long wavelengths. These theories afford more accurate treatment of ultrasonic attenuation than they do of thermal conductivity. Moreover, magnetic scattering relaxation time may be derived from ultrasonic attenuation: Phonon damping in spin interactions has the rate

$$\tau_M^{-1}(\lambda, \vec{q}) = v\,\alpha(\lambda, \vec{q}),$$

where α is the ultrasonic attenuation and v is the sound velocity. Calculations have been made of ultrasonic attenuation at longer wavelengths using mode-mode coupling techniques of Laramore and Kadanoff,[12] and by Kawasaki.[13] These calculations yield a model for τ_M^{-1} that shall be explored in terms of thermal conductivity.

Development of the ultrasonic attenuation begins with the isotropic Heisenberg hamiltonian, as treated by Stern:[14]

$$H = \tfrac{1}{2} \sum_{i,j} J(\vec{\delta}_{i,j} + \vec{u}_j - \vec{u}_i)\, \vec{S}_i \cdot \vec{S}_j \qquad (4)$$

J is the exchange interaction, $\vec{u}_i$ is the displacement of the $i^{\underline{th}}$ particle from the $i^{\underline{th}}$ lattice site, and $\vec{\delta}_{i,j}$ is the vector displacement of site j from site i.

A three-dimensional Taylor's series expansion of J is made about $\vec{\delta}_{ij}$:

$$J(\vec{u}_{ij}+\vec{\delta}_{ij}) = \sum_{n=0}^{\infty} \frac{1}{n!}\left[\vec{u}_{ij}\cdot\nabla\right]^{n}_{\vec{r}=\vec{\delta}_{ij}} J$$

where

$$\vec{u}_{ij} = \vec{u}_j - \vec{u}_i, \text{ and } \nabla = \nabla r \frac{\partial}{\partial r} = \vec{n}_{ij}\frac{\partial}{\partial r},$$

$\vec{n}_{ij} = \dfrac{\vec{\delta}_{ij}}{\delta_{ij}}$ being a unit vector from site i toward site j.

Thus,

$$J = \sum_{n=0}^{\infty} \frac{1}{n!}\left[\vec{u}_{ij}\cdot\frac{\vec{\delta}_{ij}}{\delta_{ij}}\right]^{n} \frac{\partial^n J}{\partial r^n}\Big|_{\vec{\delta}_{ij}}$$

At low temperatures, relative displacements $\vec{u}_{ij}$ may be expected small enough that sufficient accuracy will result by keeping only three terms in the expansion. One defines the strain variables by

$$\epsilon_{ij} = \vec{u}_{ij}\cdot\frac{\vec{\delta}_{ij}}{\delta_{ij}}, \tag{5}$$

whence

$$J(\vec{u}_{ij}+\vec{\delta}_{ij}) \approx J_o(\vec{\delta}_{ij}) + \frac{\partial J}{\partial r}\epsilon_{ij} + 1/2\,\frac{\partial^2 J}{\partial r^2}\epsilon^2_{ij} \tag{6}$$

Since one is interested only in spin-phonon interactions involving the strain variables, one writes the interaction hamiltonian by Equations (4) and (6),

$$H_I \approx 1/2 \sum_{i,j}\left[\left(\frac{\partial J}{\partial r}\right)_{\delta_{ij}}\epsilon_{ij} + 1/2\left(\frac{\partial^2 J}{\partial r^2}\right)_{\delta_{ij}}\epsilon^2_{ij}\right]\vec{S}_i\cdot\vec{S}_j \tag{7}$$

This is the basis for the paper by Luthi, Moran, and Pollina,[15] on ultrasonic attenuation. Treatment begins by neglect of the second-order term in H_I, because it would lead to an unobserved ω^4 dependence

for the critical attenuation.

Let the displacement operators

$$\vec{u}_j = \sum_q \sqrt{\frac{\hbar}{2M\omega_q}}\ \vec{e}_q\, \hat{a}_q\, e^{i\vec{q}\cdot(\vec{R}_k + \vec{\delta}_{ij})}$$

be introduced, where $\hat{a}_q$ are annihilation operators, and $\vec{e}_q$ are polarization vectors of the phonons; the summation covers the first Brillouin Zone. These operators are substituted into the expression $\vec{u}_{ij} = \vec{u}_j - \vec{u}_i$, whence, through the definition for ϵ_{ij}, and Equation (7), one obtains a complex expression.

The real part of this expression, under the condition $\delta_{ij} << \lambda_q$, is the interaction hamiltonian used by Luthi, Moran, and Pollina:[15]

$$H_I = \sum_{ij} \frac{\partial J}{\partial r}\Big|_{\vec{\delta}_{ij}} \frac{1}{\delta_{ij}} \sum_q \sqrt{\frac{\hbar}{2M\omega_q}}\ (\vec{\delta}_{ij}\cdot\vec{e}_q)(\vec{q}\cdot\vec{\delta}_{ij})\left[e^{i\vec{q}\cdot\vec{R}_i}\hat{a}_q - e^{-i\vec{q}\cdot\vec{R}_i}\hat{a}_q^{\dagger}\right]\vec{S}_i\cdot\vec{S}_j$$

The critical attenuation coefficient is next presented; the derivation is based on this interaction hamiltonian, H_I.

$$\alpha = \frac{1 - e^{-\frac{\hbar\omega}{k_B T}}}{2M\hbar\omega_v} \sum_{i,j,i',j'} \int_0^{\infty} e^{-i\vec{q}\cdot\vec{\delta}_{ij}} \langle X_{ij} X_{i'j'}(t)\rangle e^{i\omega t}\, dt \qquad (8)$$

where $\langle\text{----}\rangle$ denotes the thermal average,

and $X_{ij} = \frac{1}{\delta_{ij}} \frac{\partial J}{\partial r}\Big|_{\vec{\delta}_{ij}} (\vec{\delta}_{ij}\cdot\vec{e}_q)(\vec{\delta}_{ij}\cdot\vec{q})\,\vec{S}_i\cdot\vec{S}_j.$

Now the transport coefficient, α, is basically a reciprocal mean-free path for phonons of frequency ω; as such it is jointly proportional to the number density of scatterers and the cross-section of each. This latter product is thus proportional to a space-time fourier transform of the four-spin correlation function,

$$\mathcal{G}(T, \vec{\delta}_{ij}, t) = \langle \vec{S}_i(0) \cdot \vec{S}_j(0)\, \vec{S}_{i'}(t) \cdot \vec{S}_{j'}(t) \rangle . \qquad (9)$$

This transform is reminiscent of the scattering of particles by nucleii: The scattering amplitude in the Born approximation is essentially the fourier transform of the scattering potential.

It more closely parallels the concept of the dynamic structure factor, which is defined as a fourier space-time transform of a two-spin correlation function.[5] It will be recalled that this structure factor, used in connection with neutron scattering, is proportional to the spectral scattered intensity of neutrons.

A most successful but difficult evaluation of the four-spin correlation-functions has been accomplished by Kawasaki[16] and by Laramore and Kadanoff.[12] They applied mode-mode coupling theory, which uses static scaling to approximate divergent transport coefficients due to different modes of excitation, such as sound waves, heat, etc. Their evaluation of the integrals in (9) rests upon approximating assumptions, namely, that wavelengths are much longer than correlation length at the critical point ($q\xi << 1$), spin fluctuations have a time-dependence of the "hydrodynamic" form $e^{-t/\tau}{}_{ij}$, and that $\omega << \Omega_\xi$, the relaxation rate of order-parameter fluctuations for this Laremore and Kadanoff hydrodynamic regime in the paramagnetic phase. Kawasaki also used the long wavelength assumption but with the alternate assumption $\omega >> \Omega_\xi$.

The final result of calculation invoking the use of critical exponent laws for the transport parameter, α, is concisely presented by Kawasaki[17]

$$\alpha(\omega) = \frac{b_o \omega^2}{\Omega_\xi} \quad , \text{ for } \omega << \Omega_\xi \; ; \; b_o > 0.$$

This matches an earlier result by Kawasaki,[16] and by Laramore and Kada-

noff[12] for the paramagnetic phase only:

$$\alpha(\omega) \sim \frac{\omega^2 \tau}{\Omega_\xi}, \quad \text{where} \quad \Omega_\xi = |\epsilon|^p$$

is the fluctuations relaxation rate; an inverse transition lifetime. Here, $p = z - \alpha$, where z is the critical index for the relaxation rate of order parameter fluctuations, and α is the critical exponent for specific heat. It follows that

$$\frac{1}{\tau_m} \sim \frac{v\omega^2 \tau}{|\epsilon|^p}$$

in the hydro-dynamic regime.

Kawasaki's result under the alternate assumption $\omega >> \Omega_\xi$ was that

$$\alpha(\omega) \sim |T - T_c|^{\circ} \omega$$

There is a correlation length, ξ_b, which represents the boundary between the hydrodynamic regime and the critical region. The condition $q\xi_b = 1$ defines the boundary. The relevant q value is assigned by the dominant phonons: For $T = 1^\circ$ K, take $v = 2 \times 10^5$ cm/sec as the sound velocity, the wavelength as $\lambda = 30\ r_o$, where r_o is a characteristic lattice spacing of the system. One then finds a boundary correlation length

$$\xi_b \approx \frac{30\ r_o}{2\pi} \approx 5\ r_o$$

Now correlation length also follows an exponent law,

$$\xi = r_o |\epsilon|^{-\nu}$$

Assuming a value[18] $\nu = 2/3$, one finds that the hydrodynamic description may fail when

$$|\epsilon| \leq 0.09$$

Moreover, $\tau_M (T_c) = 0$, which implies, upon substitution into the Debye integral for thermal conductivity, Equation (57) in the appendix,

a vanishing thermal conductivity. This contradicts experiment, so knowledge of behavior of τ_M in the non-hydrodynamic region is essential.

2. A Semi-Empirical Model for τ_M^{-1}

There is scant knowledge of relaxation-time behavior at the boundary defined by $q\xi = 1$. Dixon, Rives, and Walton,[4] assume the Kawasaki conditions

$$q\xi < 1, \quad \Omega_\xi > \omega$$

and postulate the interpolation function (see the appendix)

$$\tau_M^{-1} = \frac{D' \omega^2 T}{C' \epsilon^p + \omega} \tag{54}$$

where

$$\Omega_\xi' = C' \epsilon^p,$$

which fits the hydrodynamic behavior for

$$\Omega_\xi' >> \omega$$

and assymptotically the Kawasaki form when

$$\omega >> \Omega_\xi'$$

This function has been used to fit the thermal conductivity measurements, with the results that for $CuK_2Cl_4 \cdot 2H_2O$ and no external magnetic field

$$p^+ = 1.56 \pm 0.10$$

$$T_c = 0.88 \text{ K} \qquad C' = (7.4 \pm 0.9) \times 10^{12} \text{ hz}$$

$$D' = 1 \text{ deg}^{-1}$$

and for $CuRb_2Cl_4 \cdot 2H_2O$,

$$p^+ = 1.72 \pm 0.2$$

$$C' = (9.1 \pm 1.8) \times 10^{12} \text{ hz}$$

and

$$D' = 0.7 \text{ deg}^{-1},$$

for the paramagnetic phase. Agreement with the theoretical value $z = 5/3$ is excellent; the logarithmic singularity in specific heat implies $\alpha \approx 0$.

A wide range of p values described the data equally well in the ferromagnetic phase in both cases: the fit was poor.

The problem here investigated is the behavior of the postulated function, τ_M^{-1}, to find the field dependence of D', and p down through the ordering temperature, $T_c = 0.88^\circ$ K for $CuK_2Cl_4 \cdot 2H_2O$, from the paramagnetic phase. The field dependence of scattering due to critical fluctuations of a few kilogauss is studied.

CHAPTER II

EXPERIMENTAL PROCEDURE

A. The Establishment of Low Temperatures

1. The Cryogenic Apparatus

a. The Cryostat and Associated Systems

Cryogenic apparatus is necessary to achieve and maintain a desired low temperature of the crystal specimen, within a degree or two of absolute zero. Also to be achieved and maintained is a known temperature gradient in the specimen. Accuracy practicable in the equipment to be described for temperature control is $\pm$ 1 millidegree.

The cryostat is an enclosure within which the specimen is suspended, and which is refrigerated by an external environment of liquid ^{4}He in this situation. The cryostat can be filled with an exchange gas, H_2 in this application, in order to cool the specimen to the outer bath temperature via the gas conductor. It can be evacuated to maximize the thermal isolation of the sample. For this purpose is provided the cryostat vacuum system.

The cryostat vacuum system consists of a mechanical forepump and a diffusion pump, arranged sequentially with valves (see Figure 1 for details of the cryogenic system) and an associated ion-gage to monitor pressure within the cryostat. The diffusion pump can be bypassed if high vacuum is not desired. Typically pressure is reduced to between

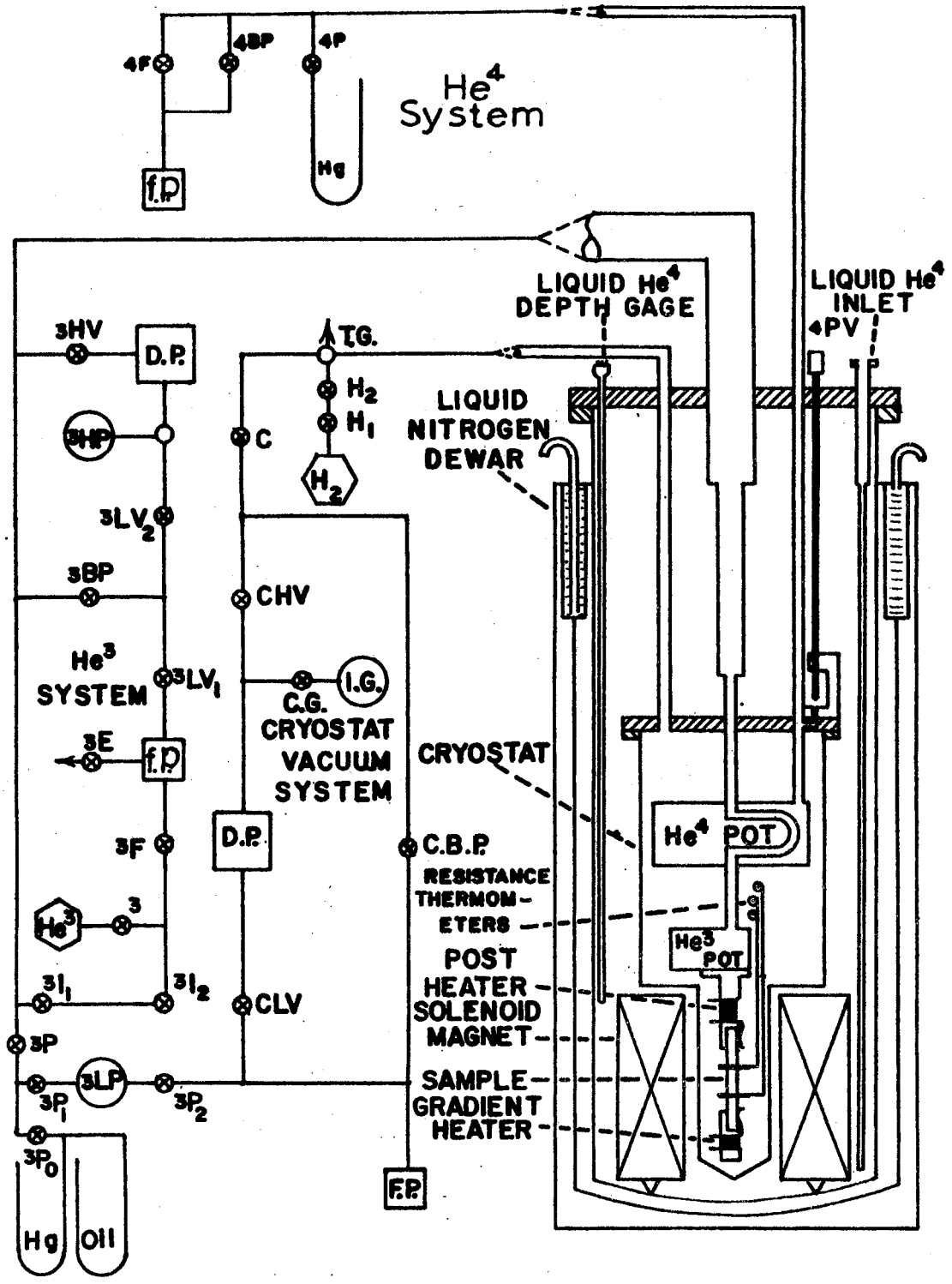

FIGURE 1. Cryogenic Apparatus

10^{-5} and 10^{-6} torr in this study.

The vacuum isolation from the external ^{4}He temperature, of the order 4.2 K, is essential before a lower temperature is possible. Advantage is taken of the lowering of the boiling-point of liquid ^{4}He under pressure reduction, to produce further cooling. A small liquid ^{4}He "pot" within the cryostat suspends another "^{3}He pot" from which the specimen is supported. (This latter pot is to be subsequently discussed). Some liquid ^{4}He is allowed to fill this ^{4}He chamber when the external liquid reaches the proper level, providing more intimate thermal contact with the specimen. Then the ^{4}He pot is "pumped down" via the ^{4}He system.

The ^{4}He system consists of a mechanical forepump with two valves in a parallel arrangement, and a mercury manometer for pressure indication. During pumpdown the liquid ^{4}He in the pot boils, its boiling point falling with the pressure, to the λ-point ($\sim$2.2 K) where ^{4}He undergoes the phase transition to the superfluid phase. After this the temperature again falls.

Previously ^{3}He gas has been admitted to the ^{3}He pot, from which the specimen is directly suspended. In the vicinity of 1.5 K, ^{3}He condenses in the tube passing through the ^{4}He pot, and runs down into the ^{3}He pot. As much liquid ^{3}He is collected as possible, while the ^{4}He pot affords some additional thermal shielding at about 1.3 K. A further temperature reduction is possible by pumping down the ^{3}He pot.

The ^{3}He system is a closed system, in which the ^{3}He is recycled to minimize its loss, since ^{3}He is an expensive by-product of hydrogen bomb manufacture. It consists of a forepump and a diffusion-pump vacuum system arranged serially, with a low pressure (3 LP) Wallace and Tiernan

gage and two parallel operated manometers (one oil and one Hg) for monitoring the pressure in the ^{3}He pot. A ^{3}He tank can supply this pressure initially through the input vales 3, $3I_1$, and $3I_2$ in the event that gas has been lost from the system. There is a fore-pressure thermocouple gage (3 HP) that reads the fore-pressure of the diffusion pump, which is the low-pressure side of the forepump. The bypass valve (3 BP) returns some of the inlet gas to the forepump, bypassing the ^{3}He diffusion pump; the fraction thus bypassed permits pressure control. The added vacuum pathway through the high vacuum valve (3 HV) produces lower pressures on the liquid ^{3}He.

The vapor-pressure of liquid ^{3}He read on the Wallace and Tiernan gage (3 LP) yields the temperature of the ^{3}He pot, and hence also of the specimen in the absence of electrical heating, via standard temperature-vapor pressure tables for liquid ^{3}He.[19] The smallest pressure division, 0.2 torr, corresponds on the average to a millidegree temperature increment.

b. Thermometry

(I). The Sample Heaters. The time-lag between pressure adjustment and thermal equilibrium, signified by steady readings in the foregoing equipment, makes the procedure awkward and difficult, if dependent only upon such adjustments. Therefore a post-heater is introduced: a resistance coil of 500 Ω on the support between the specimen and the ^{3}He pot. It is fed from the variable tap on a 1 K heliopot, which in turn is energized by a 1.5-volt dry cell, so that it dissipates between 0 and 4.5 mw of heat. One achieves thermal equilibrium near a desired temperature by adjusting the cryogenic equipment for a slow

cooling rate through the temperature, then energizing the post-heater for a compensating warming rate, as indicated by the resistance thermometer. A steady reading of the resistance R(T) of the element (A Speer carbon resistor) used as a thermometer, implies thermal equilibrium at the corresponding temperature, T.

Determination of thermal conductivity demands the creation of an easily measured temperature-gradient in the sample. This necessitates a gradient heater at the lower end of the sample. It consists of a 75 Ω coil of number 34 karma wire, whose resistance is independent of temperature. This coil is in series with a 1.5 volt cell, a variable resistance, and a standard resistor, 100 Ω. The voltage across the standard is measured to within 0.1 mv by a digital voltmeter, so that one is essentially measuring the current in the circuit: The reading in millivolts is 100 times the current in ma, I_h. One therefore knows the heat input to the crystal from the gradient heater: $I_h^2 R_h$, conviently expressed in milliwatts.

(II). <u>The Thermometers</u>. The temperature gradient is measured in terms of a resistance differential between two calibrated resistance thermometers. These are thermally anchored by clamps at a known separation, L, on the sample. The thermometers are all mounted on copper stalks to remove them as much as is convenient from the magnetic field, and thus reduce magneto resistive effects. Thermometer leads are all coiled to make them long, and of AWG # 40 manganin wire. Also, they are all anchored thermally to the ^{3}He pot, to minimize temperature differences across them. These provisions minimize conductive heat losses from the thermometers.

The thermometers are all Speer carbon resistors nominally 470 Ω,

1/2 W at room temperature. Three were carefully selected from a collection, to have nearly the same resistance at liquid helium temperature--in this case 1135Ω. These were installed in the cryostat, and calibrated via the ^3He vapor-pressure tables[19] down to 0.67 K. Further calibration down to 0.218 K was accomplished through susceptibility measurements of a $2Ce(NO_3)_3 \cdot 3Mg(NO_3)_2 \cdot 24\ H_2O$ pill via a mutual inductance bridge. Resistance at each temperature was determined by A.C. wheatstone bridge.

The calibration data were fitted to a fifth degree polynomial in a least-squares computer program, for each resistor. The thermometer used to measure T has a lead resistance correction: The correction is unnecessary except in calibration procedure for the ΔT thermometers, because lead resistance, R_{lead} cancels in the subtraction occurring in ΔR measurements. The program determined the coefficients in the polynomial[20]

$$T^{-1} = a_o + a_1 x + a_2 x^2 + a_3 x^3 + a_4 x^4 + a_5 x^5 = y$$

for each resistor where $X = \sqrt{R - R_{lead}}$, and also the computer was programmed to find the coefficients in the inverse fits,

$$X = a_o' + a_1' y + a_2' y^2 + a_3' y^3 + a_4' y^4 + a_5' y^5$$

for subsequent program usage.

(III). <u>The Temperature Bridges</u>. The resistance thermometers operate in A.C. wheatstone bridges to achieve important advantages as compared to D.C. bridge usage. Inadvertent thermo electric emfs have no effect on A.C. bridge balance. D.C. amplifiers without drift problems are relatively expensive. A.C. amplifiers with high gain and narrow band width are simpler to design, and they have a high signal to

noise ratio at the output. The advantageous phase sensitivity of the detector insures detection of the direction of bridge unbalance: whether the bridge setting is above or below the thermometer resistance.

The bridges are low frequency, to minimize reactance. Frequencies are not sub-multiples of 60 hz, so that powerline pickup is minimized.

It is important that the thermometer current produce negligible heat dissipation. The optimum current is found at the highest temperature of a run of data by first balancing the bridge at the lowest bridge excitation for which balance is practicable, then increasing the excitation. As long as unbalance is not observed, joule heating of the thermometers is tolerable. Sensitivity increases with increased excitation, so one brings the excitation to the threshold of observed unbalance. As the bridges are excited by constant voltage, the joule heating of the carbon resistors decreases with a lowering of temperature, which corresponds to an increase of resistance, since such resistors have a negative temperature coefficient. Thus joule heating remains tolerable.

The T-bridge circuit is shown in Figure 2. The lock-in amplifier supplies a 35 hz sinusoid for bridge excitation. The combined sensitivity of the pre-amplifier and the lock-in amplifier is typically such that a quarter of a millivolt of bridge unbalance at the input corresponds to 10 volts output. R(T) typically ranges from 1800Ω through 5000Ω for the temperature range of interest.

The ΔT bridge circuit is depicted in Figure 3. Two resistance thermometers, selected as that pair of the three chosen which are nearest alike in their resistance-temperature characteristics, are

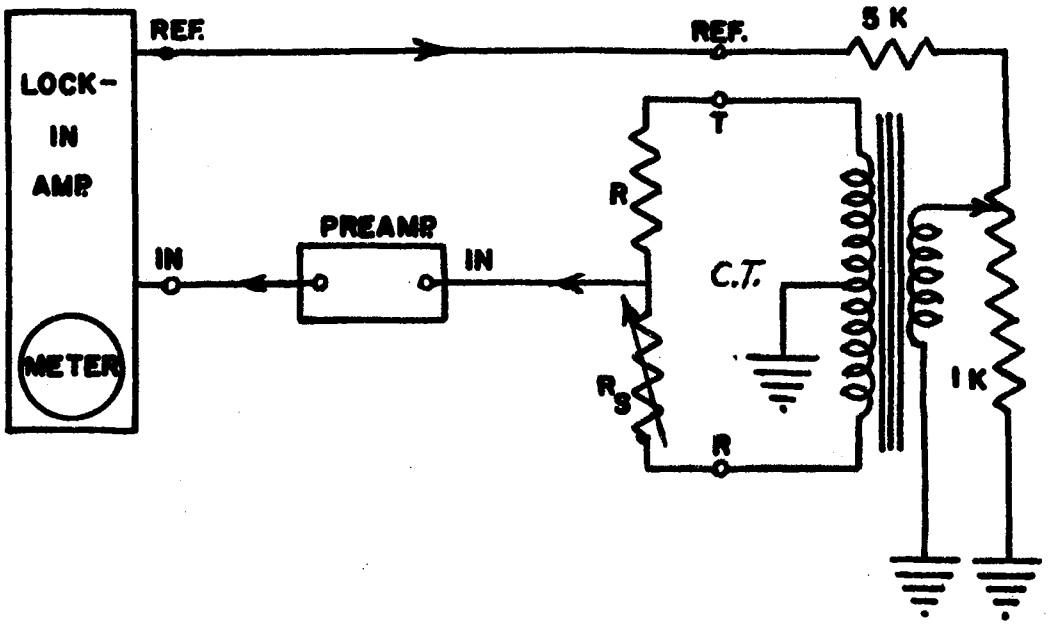

FIGURE 2. The T Bridge

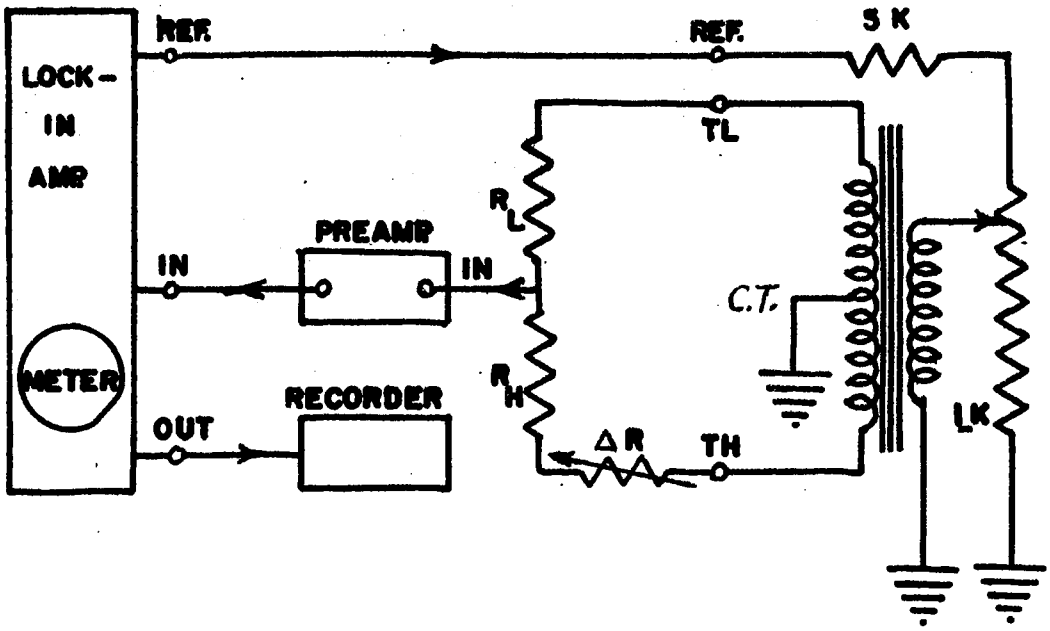

FIGURE 3. The ΔT Bridge

elements in the bridge arms. Their resistance difference diverges as their common temperature lowers; this difference, obtained without the gradient heater, is needed for getting the temperature gradient. The uniformly higher resistance, R_L, was chosen as the colder thermometer; the standard resistance, ΔR, is in series with the warmer thermometer, R_H.

A useful practice eliminated the colder thermometer in the ΔT determinations. It is only necessary to keep the temperature T (determined at the colder site), the same with the gradient heater on as it was with it off. Thus R_L remains constant, and subtracts out in the computation of δR, the desired increment in the resistance differences. At bridge balance, the standard resistance reads $\Delta R_G = R_L - R_{HG}$ with the gradient heater on, and $\Delta R = R_L - R_H$ without it, whence

$$\delta R = \Delta R_G - \Delta R = R_H - R_{HG}$$

Thus only two resistance thermometers are really used, one to measure T, the other to measure ΔT.

c. The Solenoid Magnet

A superconducting solenoid consisting of 23,815 turns of niobium base alloy wire furnishes up to 70 kilogauss at a rated current of 43.6 amperes, at 4.2 K. One derives the field at the solenoid center within $\pm$ 1% in terms of the measured magnet current, I_M: $B = 1.605\ I_M$ kilogauss.

The field is uniform within 1% over a sample volume one inch in diameter. The solenoid inductance is 18.8 henries at rated current. It has been found to remain superconducting at 75 kilogauss.

The commercial magnet power-supply permits selection of either

manual current control, or a constant sweep-rate of the current; the former was chosen in the taking of data. It features built-in safety precautions; the magnet is shunted so that inadvertent open circuits do not lead to hazardous voltages. The digital voltmeter yields magnet current in terms of the shunt voltage.

2. Cryostat Operation

a. Cooling Procedure

References to Figure 1 will facilitate understanding of the cooling process with the cryogenic apparatus.

At the outset, one evacuates the ^{3}He pot and the cryostat.

Evacuation of the ^{3}He pot really entails collecting ^{3}He on the higher-pressure side of the forepump by closing the input valve 3 I_1. Input and forepump valves, rescpectively 3 I_2 and 3 F, may be opened to allow maximum collection volume in the line. The low-vacuum valve 3 LV_1 must be opened, whence, with 3 HV closed, evacuation occurs through the opened bypass valve 3 BP. To monitor low ^{3}He pressure, the manometer gage valves 3 P, 3 P_1, and 3 P_2 are also opened.

Only the manometer valve, 4 P_1 in the ^{4}He system is open.

Cryostat evacuation requires opening of the low and high vacuum valves, CLV and CHV respectively, and the cryostat valve C. The cryostat bypass valve, CBP, and the hydrogen valves, H_1 and H_2, are closed.

One next fills the liquid nitrogen shield, at least 16 hours before a data-run. The solenoid magnet is a sizeable heat sink, and has been equipped with cooling coils; the liquid nitrogen is passed through these before entering the shield. A gold-constantan thermocouple moni-

tors roughly the magnet temperature which typically is about 120 K after a 16 hour (all night) wait.

The liquid nitrogen shield is now refilled via the magnet cooling coils, and the liquid ^{4}He pot valve is "cracked" (opened and closed), to insure it is not stuck or locked by ice. Then the ^{4}He bypass valve, 4 BP, is opened evacuating the ^{4}He pot, while the magnet and cryostat cool on down to the liquid nitrogen boiling-point, 77 K. The magnet thermocouple yields this temperature more accurately than does the resistance bridge: $R\ (77) \approx 680\,\Omega$.

Further cooling is to be accomplished with ^{4}He. Closing the cryostat vacuum valve, C, so that hydrogen can be admitted via valves H_1 and H_2 at a pressure of 1 torr as read on a thermocouple gage, prepares the system for the liquid ^{4}He transfer process.

A liquid ^{4}He transfer tube is slowly inserted into a source dewar, letting some cold gas escape to clear the tube of all but ^{4}He gas; a cloudy jet signifies sufficient precooling. The liquid ^{4}He inlet is uncorked and the transfer tube slowly inserted. Under a low pressure, cold ^{4}He gas passes up past the magnet, and cooling is monitored until the hydrogen condenses in the cryostat ($10^\circ \leq T \leq 20^\circ$), as indicated when the thermocouple gage pressure falls below 20 microns.

Upon hydrogen condensation, the transfer pressure is increased by a factor of three or four. The resistance bridge normally indicates cooling has stopped upon removal of the heat exchange gas. If not, the run is aborted, for the sample is not isolated from the ^{4}He bath.

At this point,cooling has progressed near to collection of liquid ^{4}He in the dewar. One now admits gas to the ^{3}He pot by closing the ^{3}He bypass, 3 BP, and slowly opening input valve, 3 I_1. Cooling resumes

via gas conduction.

One closes the bypass valve, 4 BP, and monitors the liquid ^{4}He depth by the level gage. Upon indication that the liquid level is above the level of the pot valve 4 PV, one opens this valve a minute, then closes. This fills the ^{4}He pot with liquid ^{4}He.

Liquid ^{4}He transfer is terminated when the level is within five inches above the valve 4 BP.

The sample temperature is now near that of the liquid ^{4}He: 4.2 K. One now further reduces temperature by "pumping down" the liquid ^{4}He in the ^{4}He pot. The bypass valve 4 BP is slowly opened, whence evaporated ^{4}He is pumped off. Pressure falls (hence also the boiling point) to the λ point, 2.186 K.

One carefully monitors the ^{3}He pressure via gage 3 LP below the λ -point. The ^{4}He cools the ^{3}He down to about 1.3 K; the ^{3}He begins condensation at about 1.7 K, corresponding to a pressure of about 40 torr. Condensed liquid accumulates in the ^{3}He pot, producing further cooling as the initially warmer ^{3}He pot revaporizes some ^{3}He to reach the temperature of liquid ^{3}He. Most condensation has occurred when the resistance bridge setting corresponds to 1.3 K.

One now closes input valve 3 I_1, and is ready for further temperature reduction via ^{3}He pumpdown.

b. Temperature Measurement

Temperature measurement without the gradient heater begins with the lock-in amplifier set for low sensitivity. One then adjusts the T-bridge until the null indicating meter is on scale; its indication is proportioned to the bridge output. One next adjusts the post heater

resistor to the midpoint of its range. This control is highly non-linear, so that heat output is a low fraction of maximum. The bypass valve, 3 BP, is now opened so that the indicator shows a slow drift-rate, preferably cooling, and near null output. Then one achieves thermal equilibrium by adjusting the post heater so that the null indicator shows a steady, on-scale reading, using increasing amplifier sensitivities. Finally, R is reset for a null reading, and the ΔT bridge is adjusted for a null output: R and ΔR are taken as data.

Temperature measurement with the gradient heator is the same, except that the gradient heater, instead of the post heater, is energized at a prescribed current before the bypass valve 3 BP is adjusted for slow cooling near null output. The post heater is then energized at little or no output, then adjusted for thermal equilibrium.

B. Thermal Conductivity Computations

The data consist of two kinds: the temperature is held constant and the field is varied, or the field is fixed and the temperature is varied. In either case, the independent variable is increased over a range of values without the gradient heater, then decreased through the same values as nearly as possible, using the gradient heater. Mismatch of corresponding values between the two sets of data is taken care of by interpolations.

Consider the gradient heater dissipation,

$$I_h^2 R_h \text{ mw.}$$

Define $T' = dT/dR$, which is found by the computer from the inverse-fit polynomial for the T thermometer. The temperature difference between thermometer clamps is then

$$\Delta T = T' \delta R.$$

Let the distance between these clamps, which has been carefully measured by a micrometer microscope, be L. If the crystal cross-section is A, then the thermal conductivity of the crystal is

$$K = \frac{I_h^2 R_h L}{A T' \delta R}$$

conveniently in milliwats (mw) per cm-degree.

I_h and δR measurements are substituted into this expression via a computer program, which also derives temperature T from R data. The program displays T, ΔT, K, and K/T^3 values.

A plot of the field dependence of the fractional change in K,

$$\frac{\Delta K}{K_o} = \frac{K_H - K_o}{K_o}$$

where $K_H = H(H, T)$, and $K_o = K(0, T)$, has the advantage of elimination of most of the measured quantities. If one keeps the gradient-heater current the same with the field on, as it was with it off, the complete factor $I_h^2 R_h L/A$ divides out in the ratio. If, in addition, the temperature is held the same in both cases, one also has $T_H' = T_o'$, and the ratio reduces to

$$\frac{\Delta K}{K_o} = \frac{\delta R_o - \delta R_H}{\delta R_H} = \frac{\delta R_o}{\delta R_H} - 1$$

A plot of this function against the field at a given temperature reveals magnetic saturation of the thermal conductivity. One may use this function and K_o derived from the zero field data, to get K_H:

$$K_H = K_o \left(1 + \frac{\Delta K}{K_o}\right)$$

This computation affords a check on computer results based on I_h values for H = 0, and is so used.

CHAPTER III

EXPERIMENTAL RESULTS

The experimental thermal average of the relaxation rate for phonon scattering due to order-parameter fluctuations, compared with the diamagnetic relaxation rate, is presented for $CuK_2Cl_4 \cdot 2H_2O$ in this chapter: $G = \langle \tau_m^{-1} \tau_o \rangle$. The data reduction is in two forms: sets of iso-champs, and sets of isotherms. The Dixon, Rives, and Walton Model[4] suggests one unknown parameter, D(H), may be eliminated to facilitate at study of the remaining parameters in the model, if the ratio of G(H, T) to $G_c(H, T_c)$, the critical isotherm, is plotted. Accordingly, isotherms of the function $\Lambda = G/G_c$ are plotted. The section following this data reduction is an attempt to relate these results to the model. The list of symbols, page viiwill expedite understanding of the sequel.

A. Data Reduction

1. Isochamps of Thermal Conductivity

The effect of fixed magnetization on the temperature dependence of thermal conductivity for $CuK_2Cl_4 \cdot 2H_2O$ is shown in Figure 4. These results show a pronounced inflection in the thermal conductivity curve near the critical temperature, most pronounced at zero field, which tends to disappear at higher fields. More revealing (Figure 5) are those plots for which the dominating T^3 dependence is divided out:

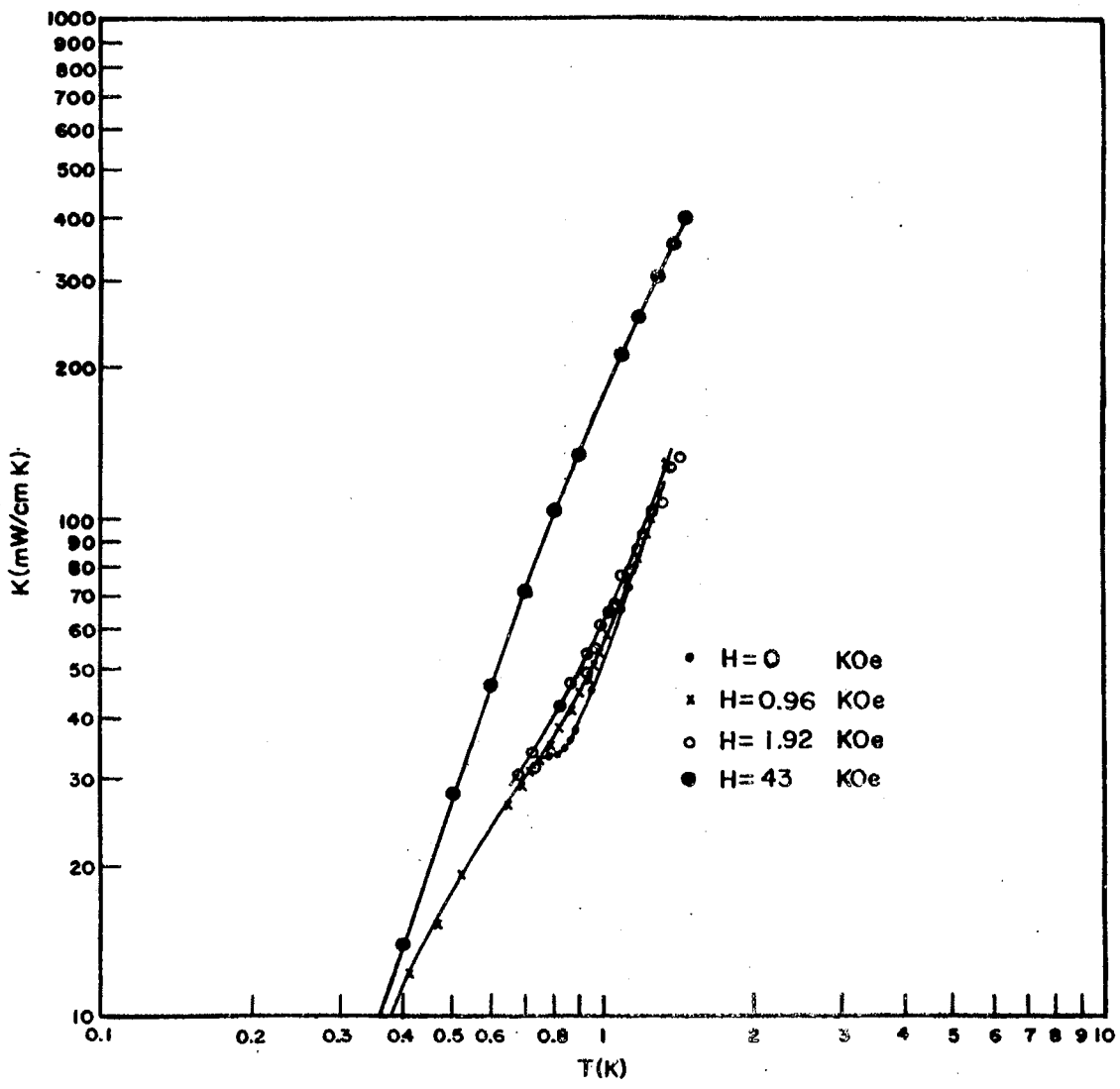

FIGURE 4. Thermal Conductivity of $CuK_2Cl_4 \cdot 2H_2O$ Through the Magnetic Phase Transition T_c = 0.88 K

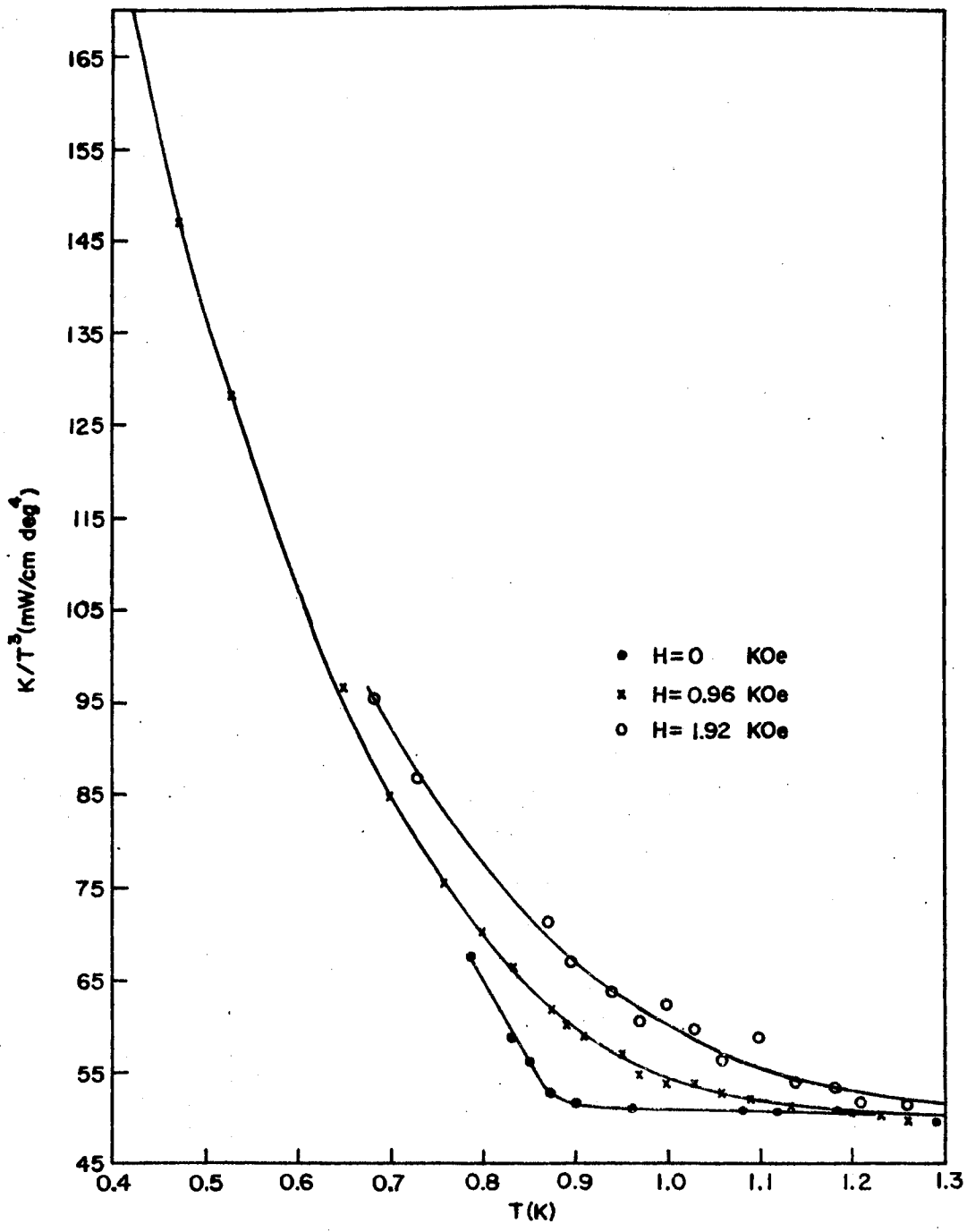

FIGURE 5. K/T^3 Plot for $CuK_2Cl_4.2H_2O$ Through the Magnetic Phase Transition T_c = 0.88 K

K/T^3 versus T at constant H. The zero-field plot appears almost to have a slope discontinuity at T_c = 0.88 K; the critical temperature is well located. For $T > T_c$, K_o/T^3, is nearly independent of T, but decreases as $T \rightarrow T_o$. The plots for $H \neq 0$ seem to show an assymptotic approach of K_H/T^3 to a minimum level as T increases above T_c.

At any given T near T_c, K_H is seen to increase with field. Since K_H depends on H only through τ_M^{-1} in the denominator of the thermal conductivity integrand (See Appendix), it follows that τ_M^{-1} has decreased. Now τ_M^{-1} is the relaxation rate for phonon scattering by low-lying excitations of the paramagnetic ions. As magnetic excitations energy increases with the field, the thermal population of excitations decreases, hence also the scattering rate decreases.

Thus the smoothing of the K(T) and K/T^3 curves in increasing field implies the reduction of the magnetic critical fluctuations: less and less phonons of the thermal distribution have sufficient energy to excite the fluctuations. A saturation field can remove the magnetic critical fluctuations entirely; this is the basis of the method for investigating the thermal average

$$G = \left\langle \frac{\tau_M^{-1}}{\tau_D^{-1}} \right\rangle$$

Under a saturation field, the thermal conductivity integral, equation (57) in the appendix, becomes

$$K_D = AT^3 \int_0^{\Theta/T} \frac{x^4 e^x}{(e^x - 1)^2} \tau_D dx; \qquad (10)$$

here, K_D is taken as a convenient symbolic way of representing $K\ (H >> K_B T/g_B)$. The total relaxation rate is $\tau^{-1} = \tau_M^{-1} + \tau_D^{-1}$, and the limiting value of τ^{-1} is τ_D^{-1} at high fields. Equation (10)

takes the numerical form

$$K_D = 9.25 \; \frac{mW}{(cmK^{\circ\,4})} \int_0^{\infty} T^3 \; \frac{x^4 e^x}{(e^x - 1)^2} \; \frac{1}{1 + 5x\,10^{-4}\, x^4\, T^4}\, dx,$$

for $CuK_2Cl_4 \cdot 2H_2O$. In practice, for this salt, fields in excess of $30KO_e$ produced saturation values of K_D.

By Equation (57) (appendix) and Equation (10) it becomes apparent that G (H, T), defined experimentally by

$$G\,(H, T) = \frac{K_D\,(T) - K\,(H, T)}{K\,(H, T)} \tag{11}$$

has the signification

$$G\,(H, T) = \frac{1}{K_H} \int_0^{H/T} \frac{x^4 e^x}{(e^x - 1)^2\,(\tau_D^{-1} + \tau_M^{-1})} \; \frac{\tau_M^{-1}}{\tau_D^{-1}}\, dx$$

i.e. $G\,(H, T) = \left\langle \frac{\tau_M^{-1}}{\tau_D^{-1}} \right\rangle_{H,T}$ according to the Debye Theory.

2. Isochamps of the Relative Magnetic Relaxation Rate, G

The function, G, is plotted versus temperature for three low-field values, Figure 6. It is seen that G (0, T) peaks at $T_c = 0.88$, implying maximum scattering rate occurs just before long-range order sets in at the critical temperature. An increase in H raises the energy required for magnetic excitations; this necessitates a rise in thermal population of higher-energy phonons before maximum scattering-rate can again occur. Thus there is a shift of G max to higher temperature as the field increases.

At the same time, the increasing order introduced by the field

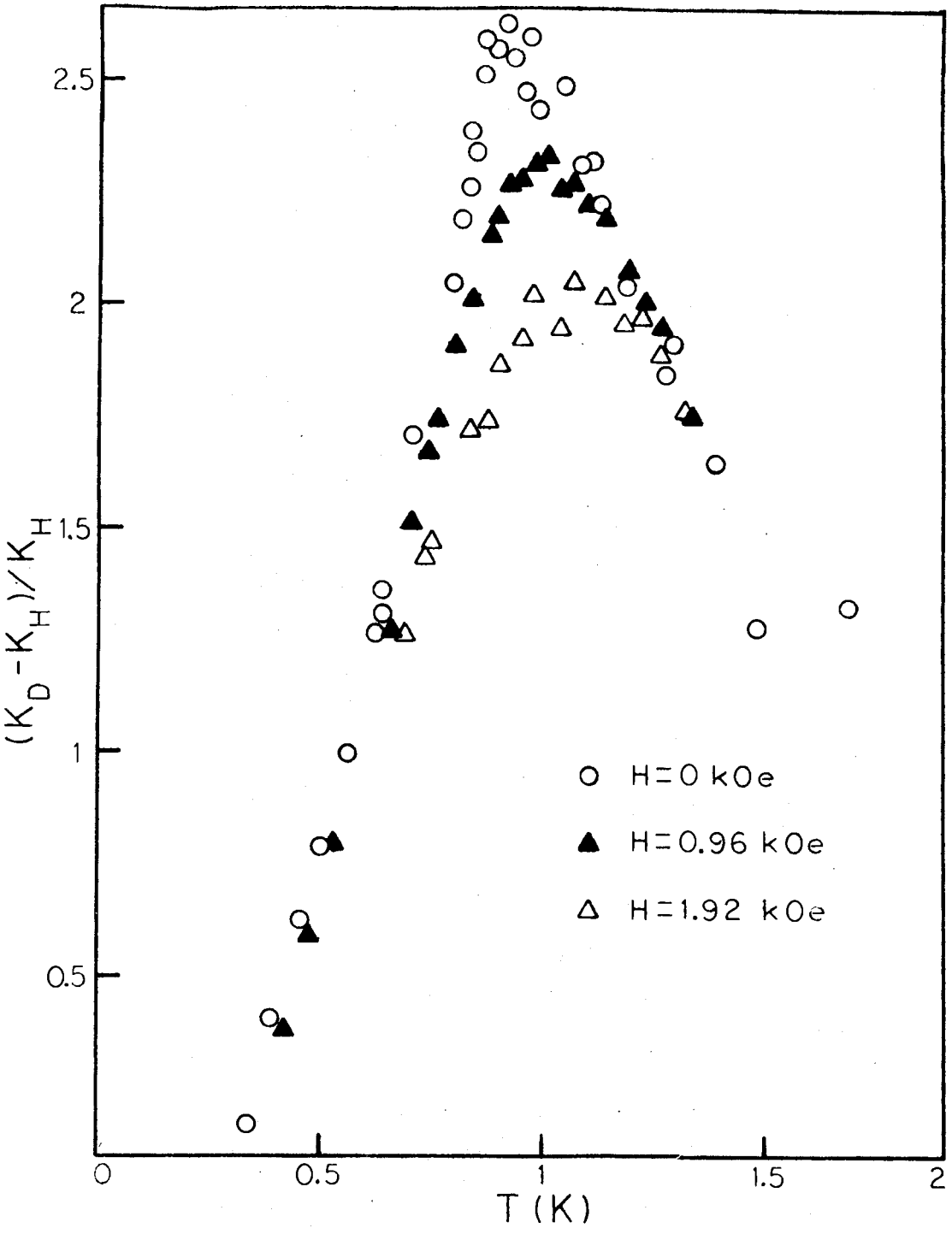

FIGURE 6. Low Field Isochamps of the Function, G

reduces the magnetic scattering rate, τ_M^{-1}, hence the peaks decrease in height.

The slope $\partial G/\partial T$ appears to be discontinuous at T_c for the two isochamps H = 0, H = 0.96 KO_e with little scatter: this clearly marks the phase transition.

These isochamps clearly behave like the magnetic specific heat, C_H, for the salt,[21] except that the zero-field specific heat is very sharp. There is one important respect in which the specific heat plots differ from these plots of the function G, however. On the high T side of T_c, specific-heat curves cross. Beyond the intersection with the $C_H(0, T)$ plot, there is a region where, for $H \neq 0$, $C_H(H,T) > C_H(0,T)$; a corresponding situation is not observed for the isochamp plots of the thermal average

$$G(H, T) = \left\langle \frac{\tau_M^{-1}}{\tau_D^{-1}} \right\rangle .$$

For further discussion of this, refer to section B, the last paragraph of part 3 in this chapter.

3. The Critical Isotherm, G_c

A log-log plot of the thermal average*,

$$G_c = \left\langle \frac{\tau_M^{-1}}{\tau_D^{-1}} \right\rangle_{T_c} = \frac{K_{Dc} - K_{Hc}}{K_{Hc}} \qquad (12)$$

computed from thermal conductivity measurements (see Appendix) is presented in Figure 7. The higher-field linearity of the plot prompted a least-squares fitting program for the function.

---

*The subscript c denotes the function at the critical temperature.

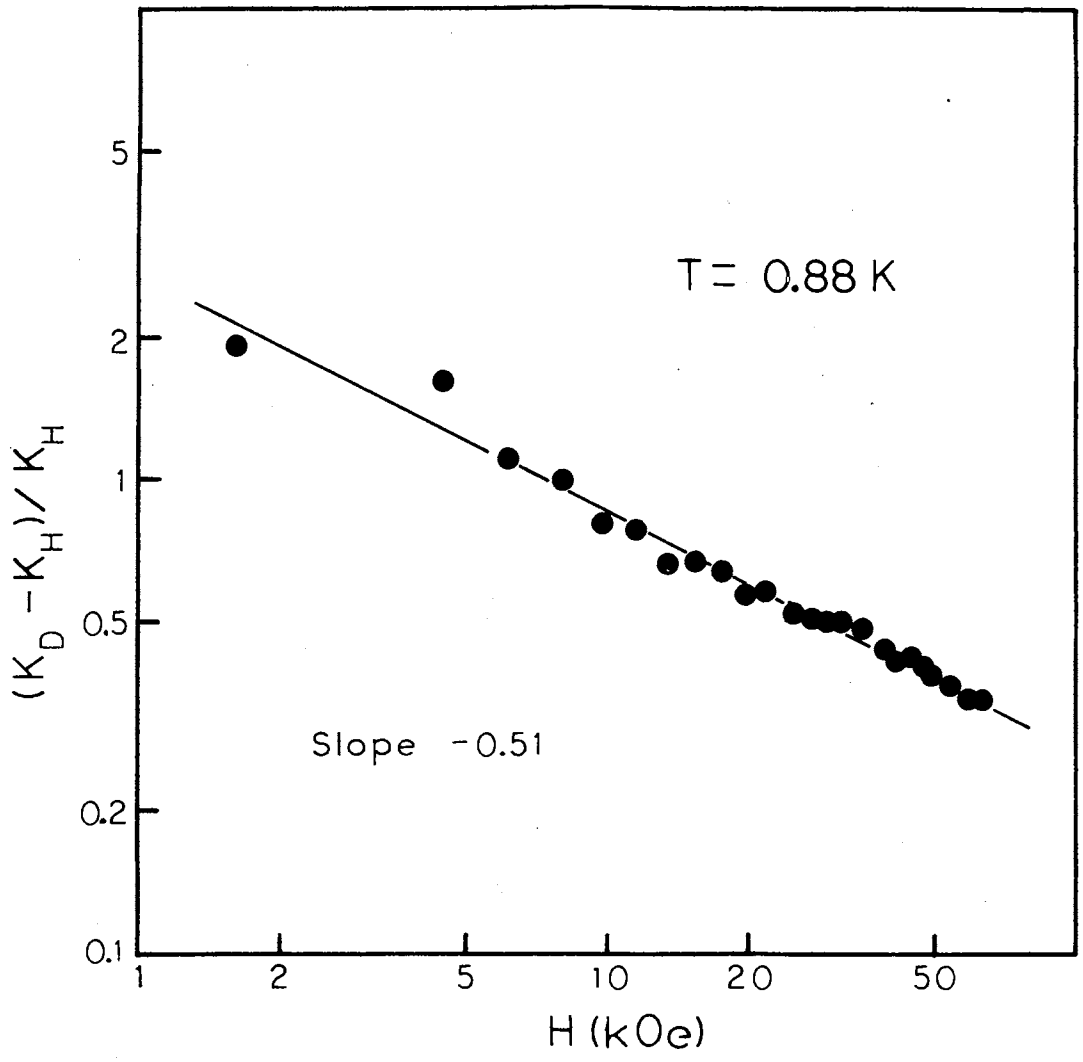

FIGURE 7. The Critical Isotherm, G_c

$$\ln G_c = \Gamma \ln H + \ln a.$$

The line of best fit had a slope $\Gamma = -0.5$, and a is a constant. At the critical temperature there is thus the power-law dependence

$$G_c = \frac{a}{H^{0.5}}$$

This function does not fit the data below 10 KOe, however. Thermal conductivity can't vanish at low fields, so a phenomenological cut-off parameter, H_{oc}, is introduced. There are theoretical grounds for a cut-off parameter[11]: Van Hove argued that the Onsager transport coefficient, Λ, depends mainly on short-range order and should remain finite at T_c. Approximate mean field calculations support the assertion. The spin diffusion coefficient satisfies the Einstein relation $\mathcal{D} = \frac{\Lambda}{\chi_M}$, where χ_M is the magnetic susceptibility, divergent at T_c. Thus $\mathcal{D}(T_c) = 0$. Then, as spin transport coefficients don't diverge for finite frequency at T_c, a cutoff parameter may be expected. Accordingly

$$G_c = \frac{a_c}{\sqrt{H_{oc} + H}} .$$

The function

$$G_c^{-2} = \frac{H_{oc} + H}{a_c^2}$$

is linear in H, with intercept $H_{oc} a_c^{-2}$, and slope a_c^{-2}. A best line was fitted to the data, G_c^{-2} versus H, Figure 8. Its intercept and slope yielded the values $H_{oc} = 1.1$ KOe, $a_c = 2.76$.

Hence,

$$G_c = \frac{2.76}{\sqrt{1.1 + H}} \qquad (13)$$

It has indeed been found[22] that more generally the function

$$G(H, T) = \frac{a(T)}{\sqrt{H_o(T) + H}} \qquad (14)$$

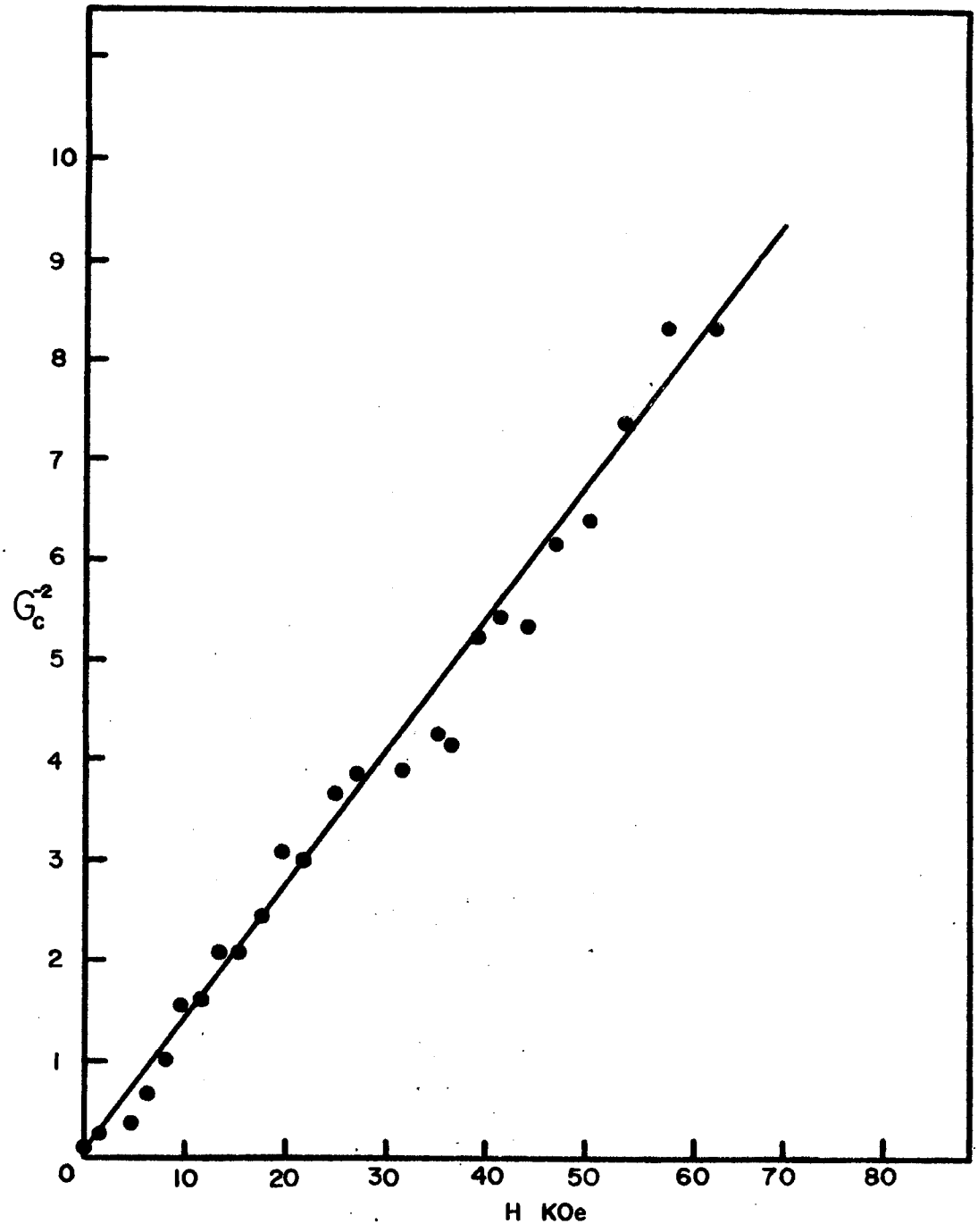

FIGURE 8. Linear Fit to G_c^{-2} (H)

G_c is the fractional change in thermal conductivity from saturation at T_c.

describes near-critical isotherms, within the bounds

$$\epsilon = \left| \frac{T}{T_c} - 1 \right| < 10^{-1}.$$

the uncertainties in the exponent Γ for G_c, for the cutoff parameter $H_o(T)$, and for the parameter $a(T)$ are $\pm$ 12%.

4. Isotherms of the Hydrodynamic Regime

Initial attempts to plot the function

$$\Lambda = \frac{\langle \tau_M^{-1} \ \tau_D \rangle_T}{\langle \tau_M^{-1} \ \tau_D \rangle_{T_c}} \tag{15}$$

for fixed $T \geq 1.05^{\circ}$, looked suggestive of exponential decay. This prompted plots on semilog paper of the same data. There resulted obviously linear plots for all of the isotherms for $H \geq t$ KOe, Figure 9. The plots all exhibit a rather sharp rise from $\Lambda(0, T)$, which starts between 0.6 and 0.9, to the linear portion at about 5 KOe. A comparison of the various isotherms reveals the random scatter of points fitted by the lines.

The plots fit the equation

$$\text{Log}\,\Lambda = \text{Log}\, b + m_1 H \tag{16}$$

where m_1 is the slope of the line, and b is its zero-field intercept. A best line for each temperature was constructed using statistical procedure, and extensive base 10 log tables.

Equation (16) in the form

$$\Lambda = b\, 10^{m_1 H}, \quad \text{for } H \geq 5 \text{ KOe},$$

is better described in terms of a critical exponent law which considers $10^{m_1} = \epsilon^{H_1^{-1}}$, where H_1 is a field-parameter, hopefully fixed, and

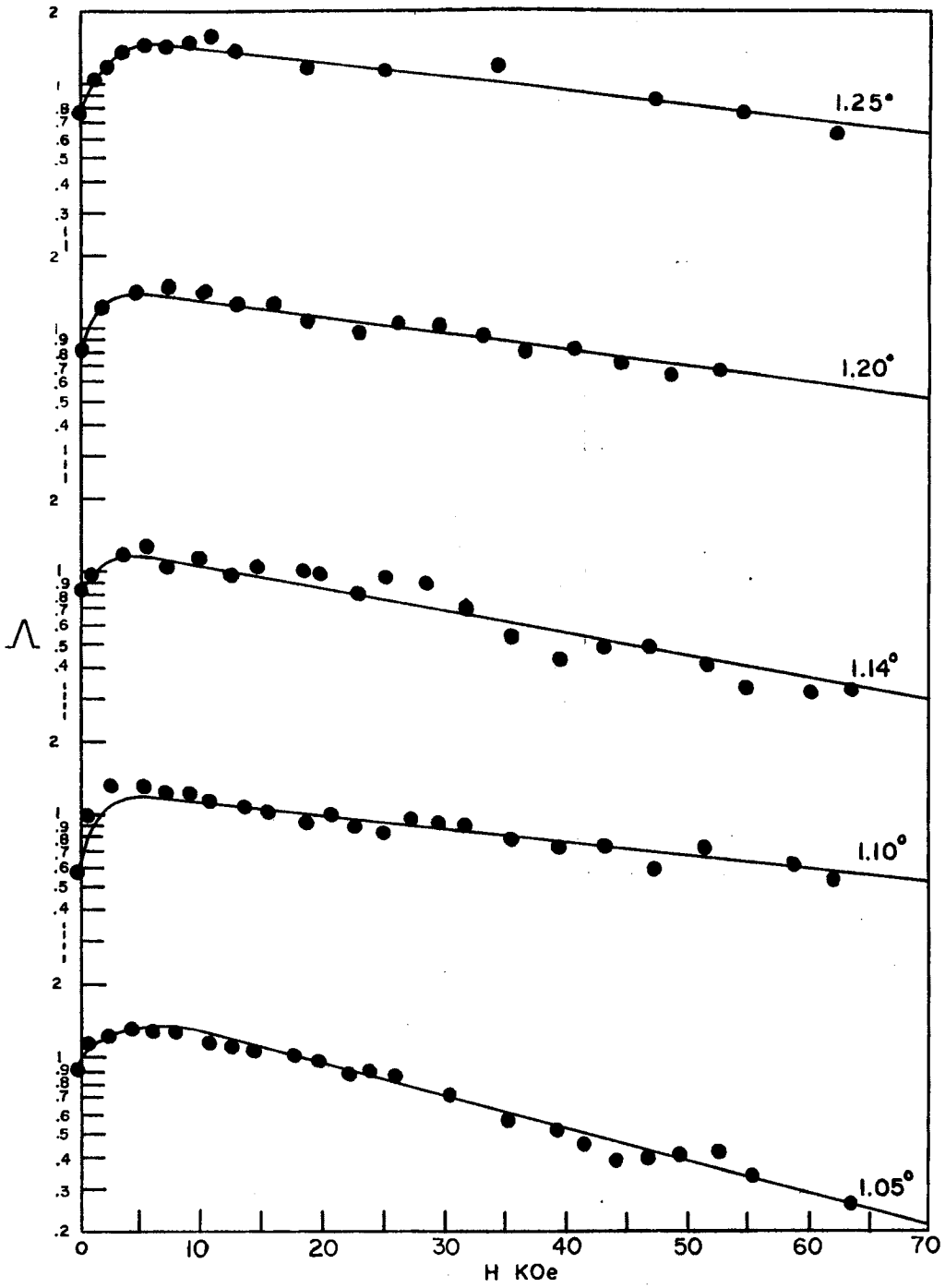

FIGURE 9. The High-Temperature Isotherms $\Lambda(H)$ for $CuK_2Cl_4 \cdot 2H_2O$

Λ is the ratio of the percentage change in thermal conductivity from saturation at T(K), to that at T_c.

$\epsilon = \left|\frac{T}{T_c} - 1\right|$. Thus

$$H_1 = \frac{\text{Log}_{10}\ \epsilon}{m_1} \tag{17}$$

Parameters from the lines of best fit are detailed in the following table:

TABLE II

PARAMETERS FOR LINEAR ISOTHERMS

T		m_1	H_1KOe	b
1.05°	.1909	-0.0128	57.15	1.80
1.11°	.2614	-0.00504	115.7	1.29
1.14°	.2954	-0.00878	60.3	1.30
1.20°	.3625	-0.00637	69.1	1.49
1.25°	.4194	-0.00582	64.9	1.61

The values of H_1 in the table, apart from the very divergent one at 1.11°, appear to be randomly distributed around an average, this average being $\overline{H}_1$ = 62.6 KOe. The slopes of the semilog plots, if T dependent, should have a monotonic dependence on T; the plots show no evidence of this. The inescapable conclusion, is that H_1 indeed is constant, and that the various values of H_1 reflect systematic errors

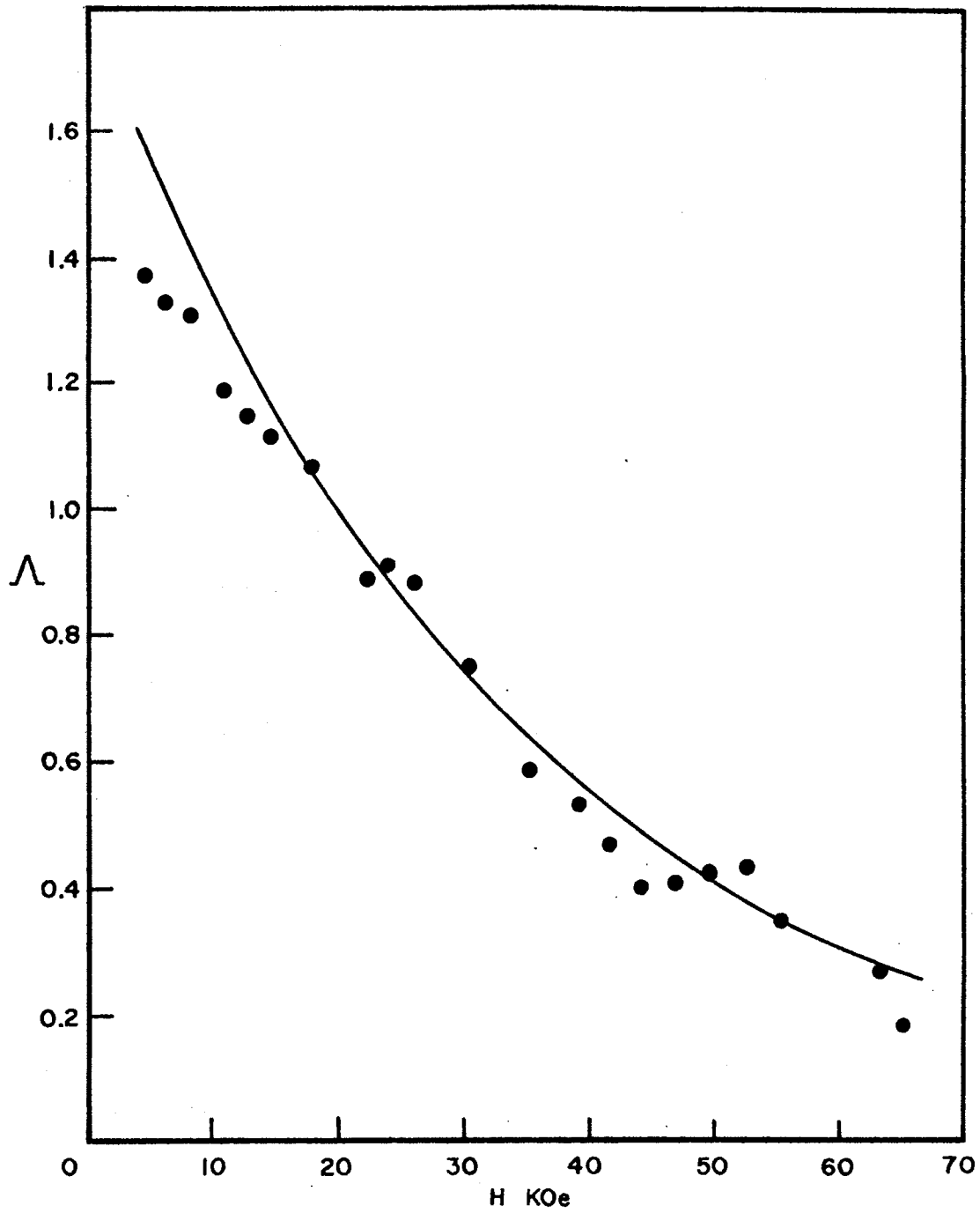

FIGURE 10. The Isotherm $\Lambda(H, 1.05^{o})$ for $CuK_2Cl_4.2H_2O$

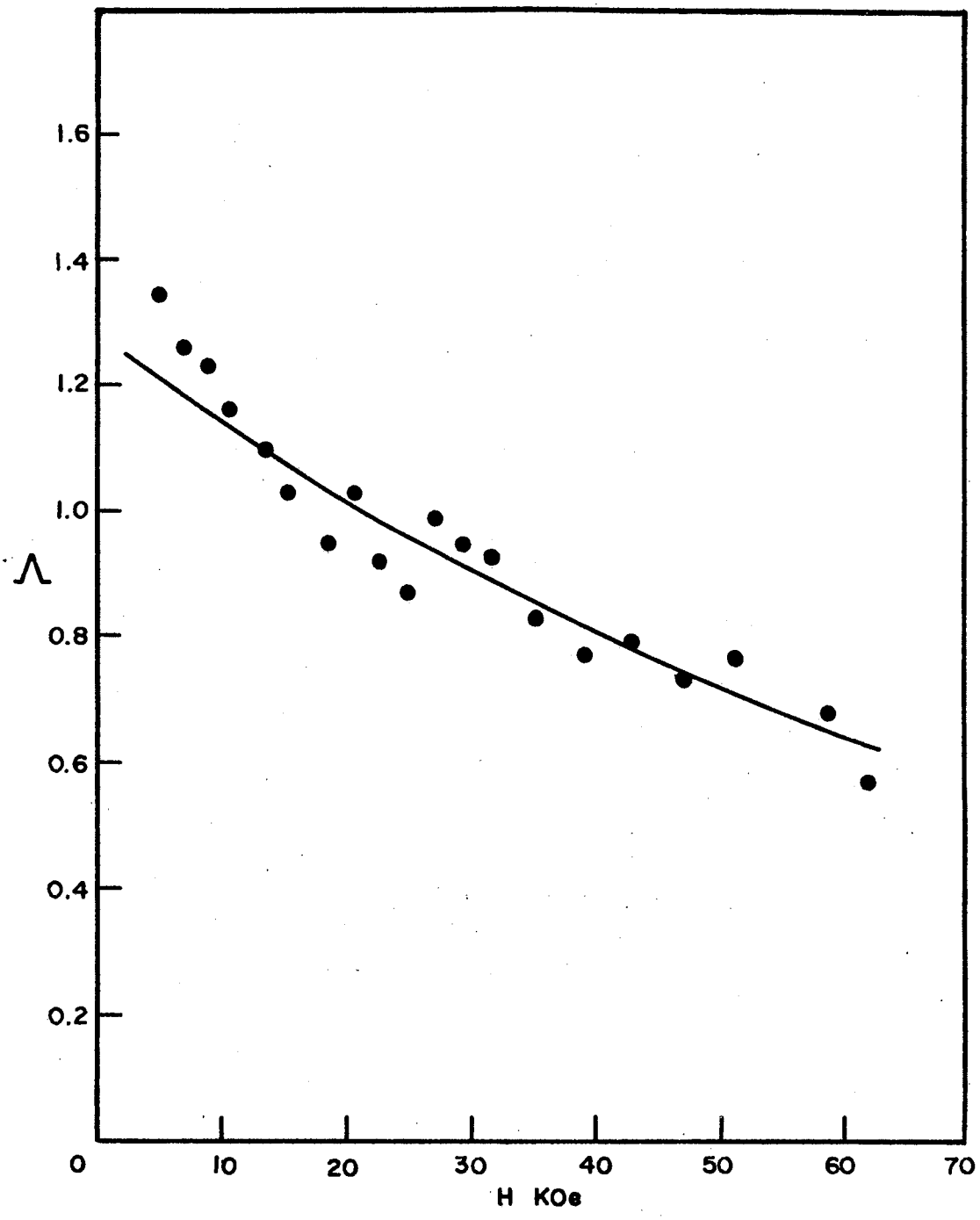

FIGURE 11. The Isotherm $\Lambda(H, 1.11^{o})$ for $CuK_2Cl_4 \cdot 2H_2O$

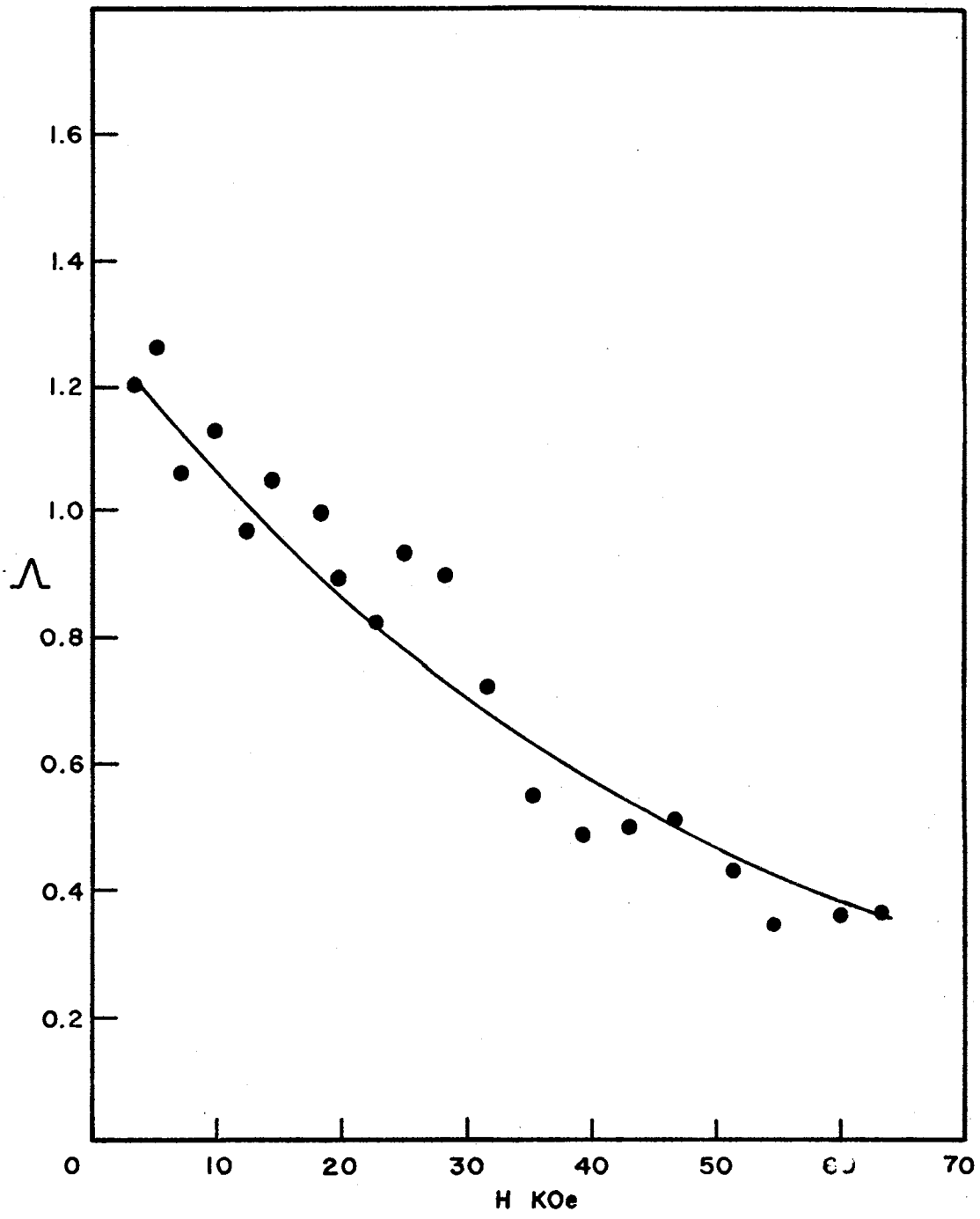

FIGURE 12. The Isotherm $\Lambda(H, 1.14^{o})$ for $CuK_2Cl_4.2H_2O$

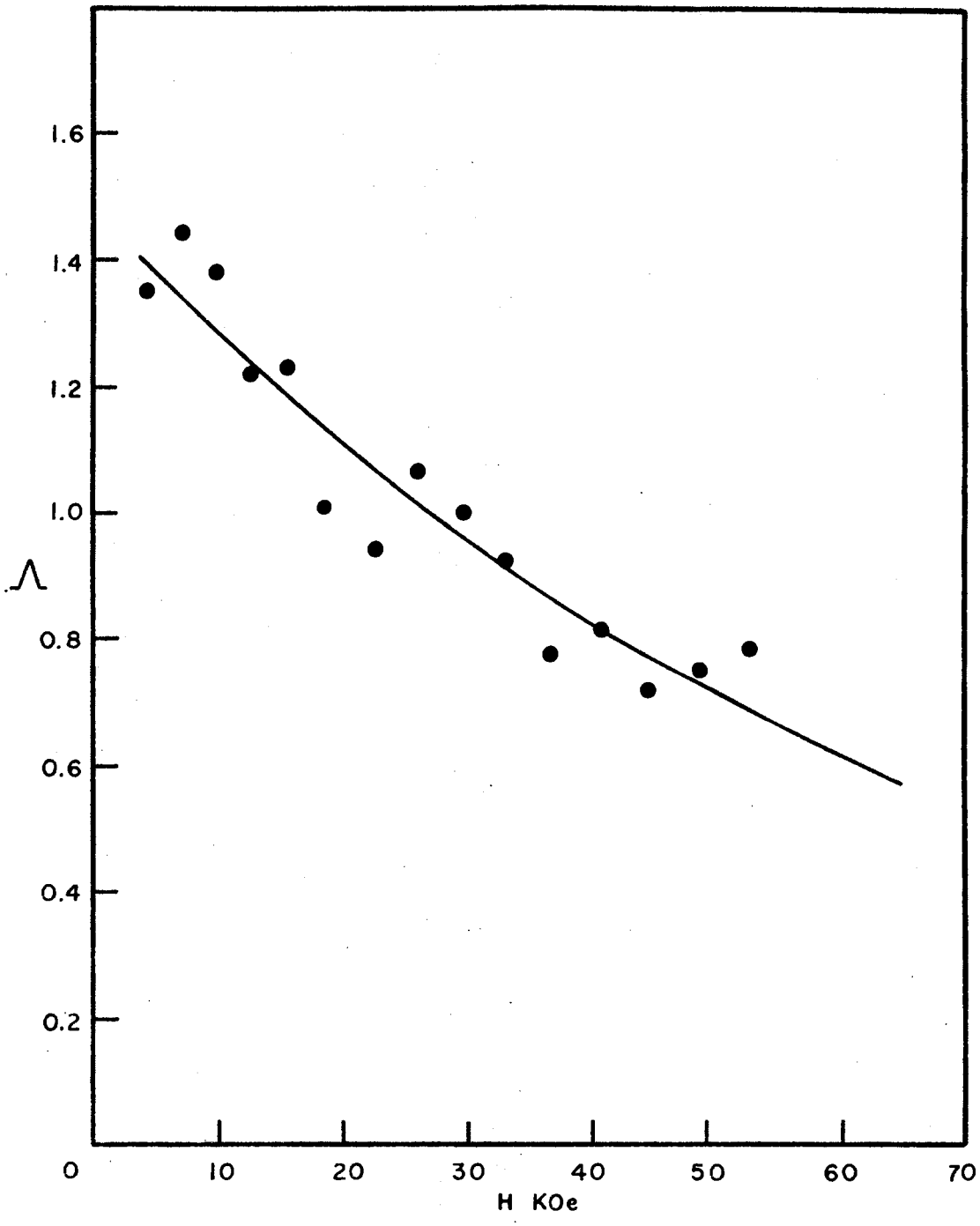

FIGURE 13. The Isotherm $\Lambda(H, 1.20^{o})$ for $CuK_2Cl_4 \cdot 2H_2O$

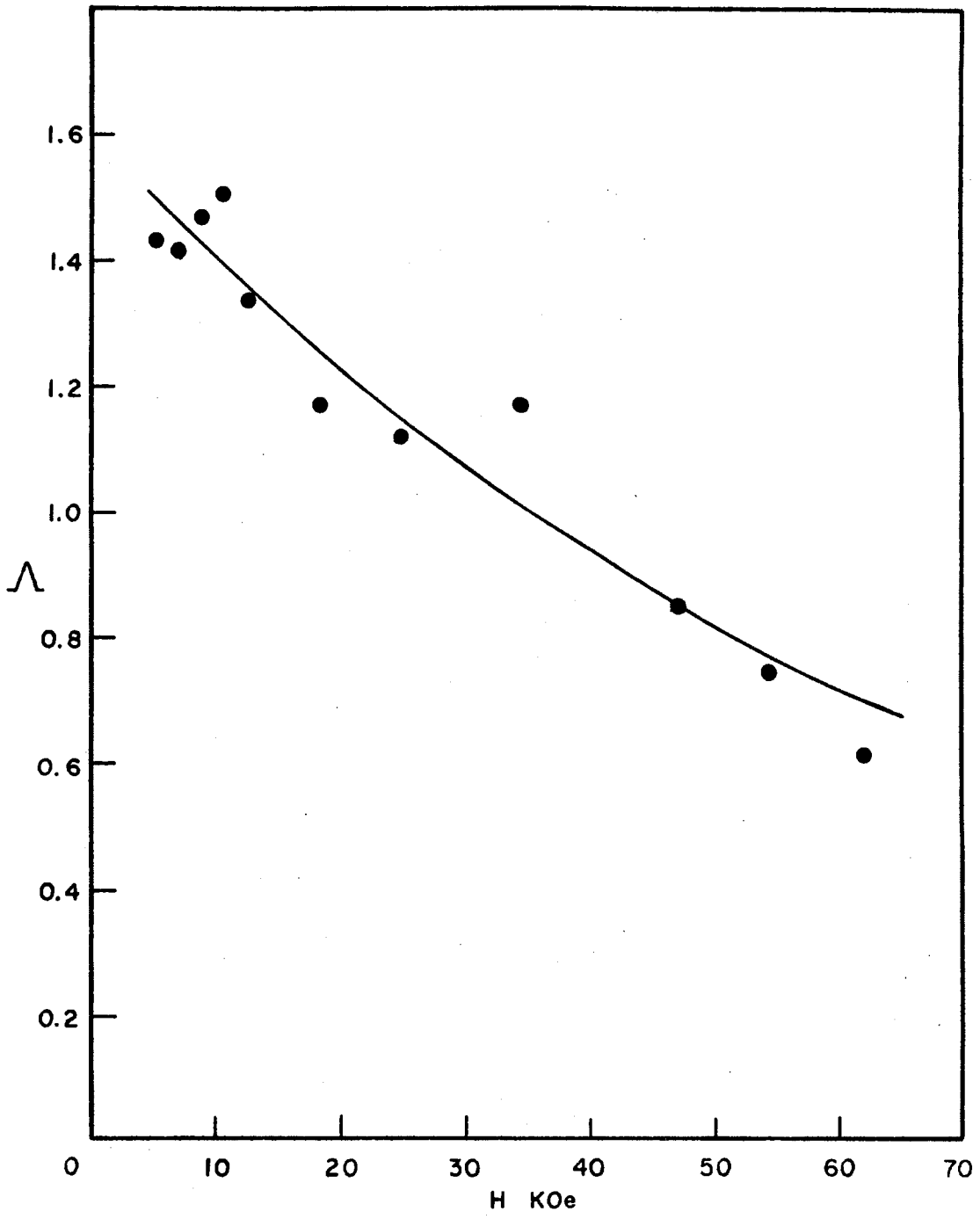

FIGURE 14. The Isotherm $\Lambda(H, 1.25^{o})$ for $CuK_2Cl_4.2H_2O$

in the data runs.

The best fit to each isotherm, Λ versus H, is depicted in respective Figures 10, 11, 12, 13, and 14, as a solid curve abouve 5 KOe in each plot of data. Each was computed according to the equation

$$\Lambda = b\epsilon^{H/H_1}$$

It is concluded that the isotherms of the hydrodynamic regime, $T \geq 1.05^{o}$, fit the critical exponent law

$$\Lambda = b\epsilon^{H/\bar{H}_1}, \qquad (18)$$

for $H \geq 5$ KOe, and $\bar{H}_1 = 62.6$ KOe.

The systematic error in a data-run probably dervies from knowing the field to an accuracy of 1% or to less accuracy. It is quite likely that residual field is responsible for a slope error.

5. Isotherms of the Critical Region

A family of three relative isotherms, $\Lambda = G/G_c$, presented in Figures 15, 16, and 17, exhibit the behavior of the average magnetic scattering relaxation rate in the critical region:

$$\Lambda = \frac{\langle \tau_M^{-1} \tau_D \rangle_T}{\langle \tau_M^{-1} \tau_D \rangle_{T_c}} .$$

The gap at 37 KOe in Figure 16 corresponds to a slight heater-current drop that occurred during the data run; the fractional change in thermal conductivity, $\Delta K/K_o$, shows a corresponding gap associated with some inadvertent change in a circuit parameter.

All isotherms plotted, for $T > T_c$ and $T < T_c$, exhibit the common feature of a sharp rise in the mean magnetic scattering rate from 0 to about 5 KOe. The rise is sharper at T near T_c. Data is sufficient for

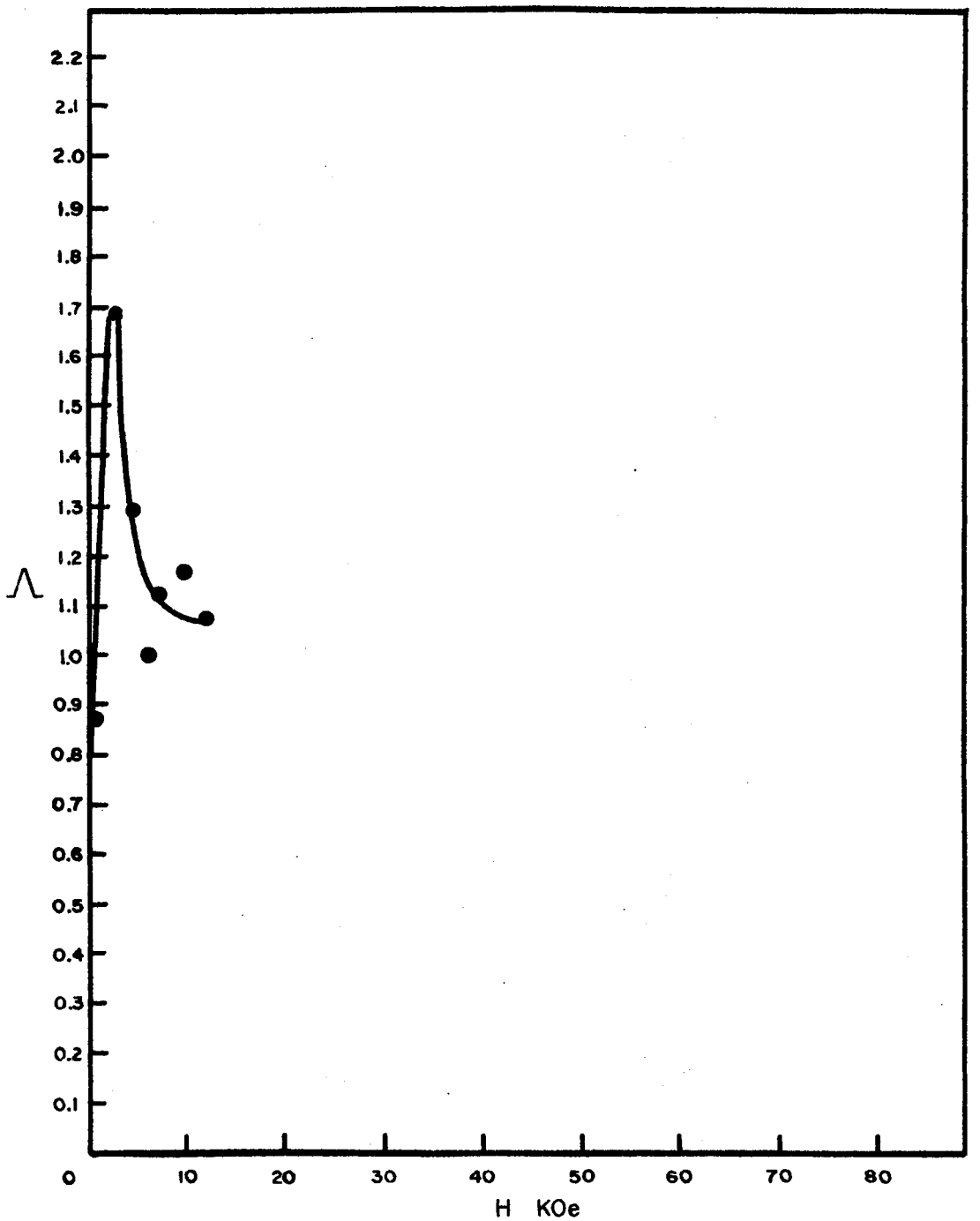

FIGURE 15. An Isotherm in the Ferromagnetic Phase, $\Lambda(H, 0.67^{o})$, for $CuK_2Cl_4.2H_2O$

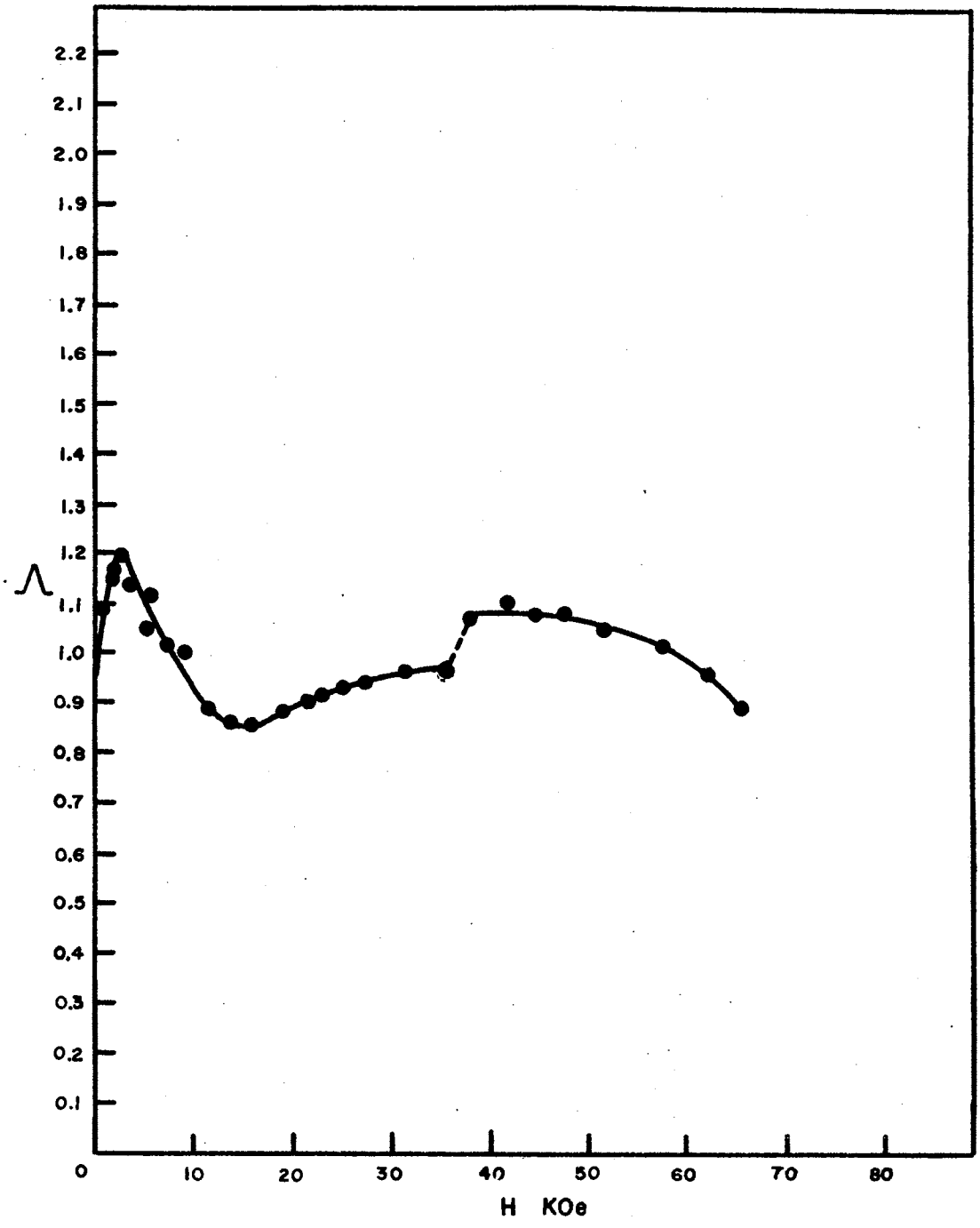

FIGURE 16. An Isotherm in the Ferromagnetic Phase, $\Lambda(H, 0.815^{\circ})$, for $CuK_2Cl_4.2H_2O$

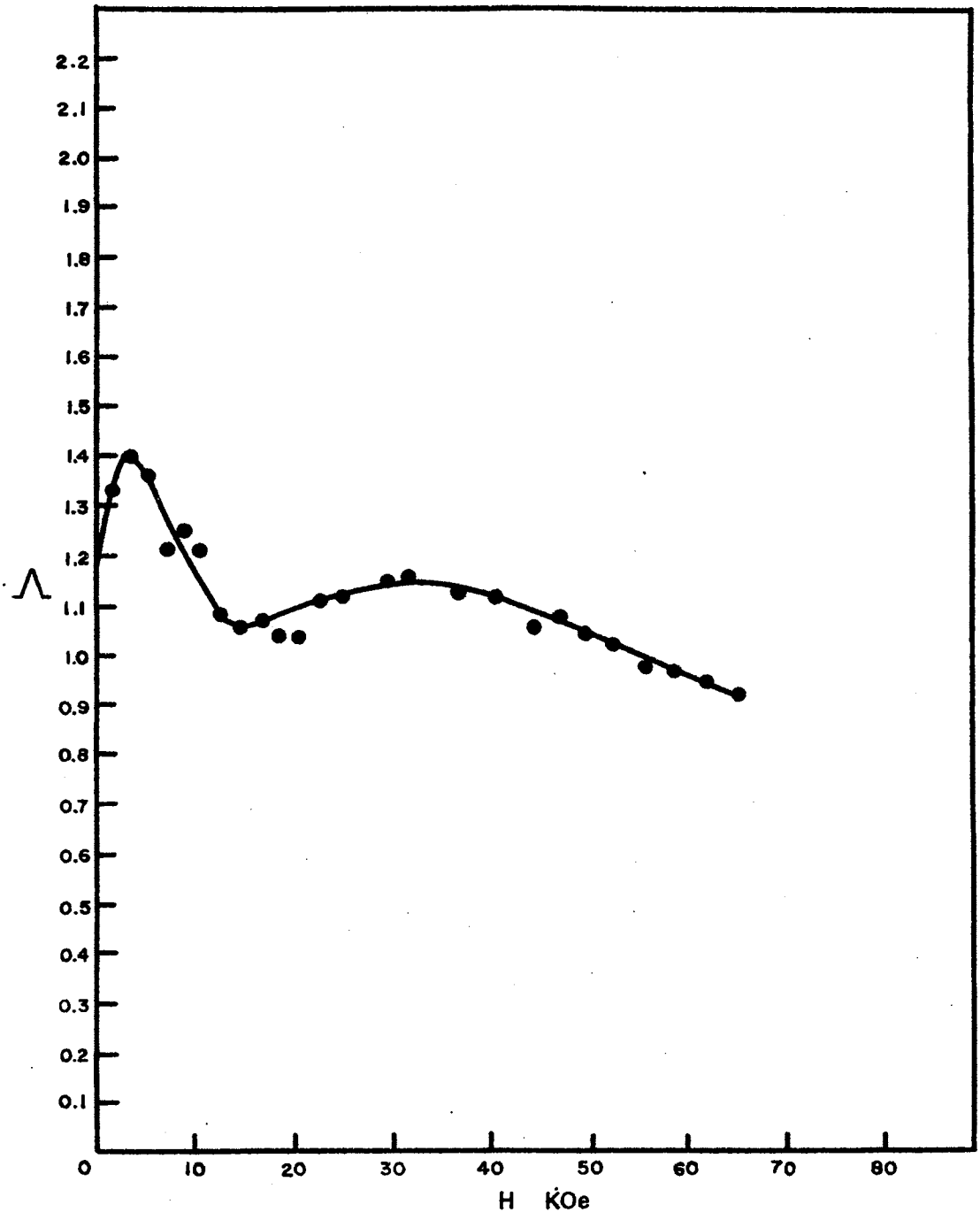

FIGURE 17. The Critical-Region Isotherm $\Lambda(H, 0.96^{o})$ for $CuK_2Cl_4 \cdot 2H_2O$

the 0.67° isotherm to indicate a very sharp peak; the peak appears to broaden a little as T rises past T_c.

It must be admitted that in view of the inadequate theoretical treatment to date of the relaxation rate τ_M^{-1}, this feature is not understood. The two isotherms of the critical region, Figures 16 and 17, brackett T_c, showing that the behavior of Λ above and below but near T_c is similar.

These isotherms of the critical region show that the mean magnetic scattering relaxation rate for phonons sharply peaks a little below 5 KOe, starting from a relatively low rate at H = 0. The zero-field intercept rises with temperature. The relative rate Λ falls to a minimum at about 15 KOe, then rises slowly to a maximum at about 40 KOe for 0.82°, at 35 KOe for 0.96°.

The isotherms of the critical region superficially resemble two-term exponential plots. This in turn is suggestive of critical exponent terms. Following the hint, the Dixon and Walton Model[4] is expressed in terms of a thermal average dependent on the sum of two terms, in the data analysis.

B. Data Analysis

The interpolation model for the relative magnetic relaxation rate Equations (54) and (56) (see the Appendix) is here developed in a form that can be studied in terms of the data reduction of section A. Thus the function G is, according to the model.

$$G(H, T) = D(H, T) \left\langle \frac{x^2 T^3}{\tau_D^{-1} (\Omega + xT)} \right\rangle_T$$

Allowance for the possibility of T-dependence of D is made, though D (H) was assumed in the original model. One can multiply the numerator and

the denominator of the fraction by τ_D/xT, and then factor out T^2 to get

$$G(H, T) = D(H, T)\, T^2 \left\langle \frac{x\tau_D}{\frac{\Omega}{xT} + 1} \right\rangle_T \qquad (19)$$

It is convenient to define the parameter $y = \frac{\Omega}{xT}$,

whence

$$G(H, T) = D(H, T)\, T^2 \left\langle \frac{x\tau_D}{1 + y} \right\rangle_T \qquad (20)$$

The manner in which this expression of the model becomes experimentally accessible is developed in the sequel.

1. Significance of the Critical Isotherm, G_c

At the critical point, the rate of magnetic-ordering fluctuations vanishes: $y = 0$. Then the model yields

$$G_c = D(H, T_c)\, T_c^2 \langle x\tau_D \rangle_{T_c} \qquad (21)$$

This is equivalent to the empirical Equation (13), whence one derives the critical coupling coefficient

$$D(H, T_c) = \frac{a_c}{T_c^2 \langle x\tau_D \rangle_{T_c} \sqrt{H_{oc} + H}} \qquad (22)$$

where $a_c = 2.76$, $H_{oc} = 1.1$ KOe.

It is thus seen that this coefficient exhibits the inverse square-root law.

Moreover, the fact that Equation (14) has the same form as that of G_c (Equation (13)) in the critical region for $\epsilon < 10^{-1}$ implies

$$\left\langle \frac{x\tau_D}{1 + y} \right\rangle_T \approx \langle x\tau_D \rangle_T$$

within the accuracy of the plots. This condition on Equation (20), combined with Equation (14), implies a square-root law for the coupling coefficient in the critical region:

$$D(H, T) = \frac{a(T)}{T^2 \langle x\tau_D \rangle_T \sqrt{H_o + H}} . \qquad (23)$$

The cutoff field, H_o, and the function a, are T-dependent, thus revealing D to be temperature dependent, as suspected.

But Equation (21) can be placed in simpler form. Consider the report by Dixon, Rives, and Walton,[4] on fitting the interpolation formula to a plot of the difference between zero-field conductivity and that calculated with only background scattering. Assuming $\Delta = C(H)\epsilon^P$; D, C, and P were taken as adjustable parameters. A best fit was achieved* with $D'(0, T) = 1\ \text{deg}^{-1}$. (The other parameters for $CuK_2Cl_4 \cdot 2H_2O$ are listed at the end of Chapter I). Assuming this value, a simple ratio shows, by Equation (22),

$$\frac{D(H, T_c)}{D(0, T_c)} = \sqrt{\frac{H_{oc}}{H_{oc} + H}} = \frac{D'(H, T_c)}{1}, \text{ i.e.}$$

$$D'(H, T_c) = \sqrt{\frac{H_{oc}}{H_{oc} + H}} . \qquad (24)$$

2. The Model in Accessible Form

Equations (20) and(21) yield the model expression for the

---

*considering τ_B to be the boundary-scattering relaxation time, $D(H, T) = \frac{k_B}{\hbar} \tau_B D'(H, T)$. In the ratio, however, the constant divides out. See Equations (53) and (54) in the appendix.

relative isotherms, Λ :

$$\Lambda = \frac{D\,(H,\,T)}{D\,(H,\,T_c)} \left(\frac{T}{T_c}\right)^2 \frac{1}{\langle x\tau_D\rangle_{T_c}} \left\langle \frac{x\tau_D}{1+y} \right\rangle_T = \frac{G}{G_c} \tag{25}$$

These functions are meaningful only as isotherms experimentally, for the H-dependence of D is not cancelled except at T_c. Incorporating the previous results, Equations (22) and (23), we get the ratio

$$\frac{D\,(H,\,T)}{D\,(H,\,T_c)} = \frac{a}{a_c} \left(\frac{T_c}{T}\right)^2 \frac{\langle x\tau_D\rangle_{T_c}}{\langle x\tau_D\rangle_T} \sqrt{\frac{H_{oc}+H}{H_o+H}}\,. \tag{26}$$

Substitution of Equation (26) into (25) yields

$$\Lambda = \frac{a}{a_c} \sqrt{\frac{H_{oc}+H}{H_o+H}} \frac{1}{\langle x\tau_D\rangle_T} \left\langle \frac{x\tau_D}{1+y} \right\rangle_T .$$

Define

$$\Lambda_o = \frac{a\,(T)}{a_c} \sqrt{\frac{H_{oc}+H}{H_o+H}}, \tag{27}$$

whence

$$\Lambda = \frac{\Lambda_o}{\langle x\tau_D\rangle_T} \left\langle \frac{x\tau_D}{1+y} \right\rangle_T . \tag{28}$$

It remains to simplify this via the generalized mean-value theorem* of definite integrals. Consider a weighting function $I\,(H,T,X) \geq 0$, continuous on the interval of integration $0 \leq X \leq X_m$, and any other function $g\,(H,T,X)$ also continuous on this interval. The theorem then asserts

$$\int_0^{X_m} I\,(H,T,X)\; g\,(H,T,X)\; dx = g\,(H,T,\bar{X}) \int_0^{X_m} I\,dx,$$

where $\bar{X}\,(H,T)$ is some particular value of X in the interval: $0 \leq X \leq X_m$.

---

*See various advanced calculus texts: Sokolnikoff, pages 114, 115, or Courant, Differential and Integral Calculus, vol. II, (1937) p. 232.

Let I_t be the integrand of the thermal conductivity integral (see the appendix). $I_t \geq 0$, and is continuous over the interval. Consider the weighting function $I = I_t \tau_D \; X \geq 0$, and the other function $(1 + y)^{-1}$ is continuous over the interval $0 \leq X \leq X_m$. Then

$$\frac{1}{\langle x \tau_D \rangle_T} \left\langle \frac{x \tau_D}{1 + y} \right\rangle_T = \frac{\int_o^{x_m} I \, (1 + y)^{-1} \, dx}{\int_o^{x_m} I \, dx} = \frac{1}{1 + z} \tag{29}$$

with $Z = \dfrac{\Omega}{\bar{X}T}$, and $0 \leq \bar{X} \, (H, T) \leq X_m$.

Now $\bar{X}T = \hbar\bar{\omega}/k_B$ where $\bar{\omega}$ denotes an average frequency of the phonon distribution. One sees Equation (56) (in the appendix) that

$$Z = \frac{\Omega}{\bar{X}T} = \frac{\Omega'}{\bar{\omega}}, \tag{30}$$

which is to be understood as a regime index, according to the ordering relations $Z >> 1$, (hydrodynamic), or $Z << 1$ (non-hydrodynamic). (See the end of Chapter I). In terms of this regime index, the function Λ takes a rather simple form

$$\Lambda = \frac{\Lambda_o}{1 + Z} \tag{31}$$

by Equations (28) and 29).

3. Hydrodynamic Isotherms According to the Model

The average relative magnetic relaxation rate, Λ, has been seen to fit a critical exponent law involving a single term, for $T \geq 1.1^o$ and $H \geq 5$ KOe. The interpolation model must then yield such a critical exponent law in this domain, to fit experiment. The model for the rate of order-parameter fluctuations (see the discussion associated with Equation (56) in the appendix) is here assumed of the general form

$$\Omega' = C' \, (H, T) \epsilon^{\lambda(H, T)} \tag{32}$$

The reason for allowing the possibility of dependence of the exponent on T is this: the exponent is not known in the subcritical regime, nor for $H \neq 0$ in the hydrodynamic regime. Dixon, Rives, and Walton,[4] found the value $\lambda(0, T) = 1.56 = p$, a constant for the paramagnetic phase but any choice, p' of exponent within the domain $1 \leq p' \leq 4$ fitted equally well the ferromagnetic phase of $CuK_2Cl_4 \cdot 2H_2O$. It seems prudent also to regard C' to be T-dependent until experimentally proven not so, if not.

The regime index accordingly follows a critical exponent law

$$Z = \frac{C'(H, T)\epsilon^{\lambda(H, T)}}{\omega}$$

The condition that Equation (31) can represent the desired critical exponent law is then that $Z \gg 1$, which sets the hydrodynamic regime for sufficiently high ϵ, so that

$$\Lambda \approx \Lambda_0 Z^{-1} = \frac{\Lambda_0 \omega}{C'(H, T)} \epsilon^{-\lambda(H, T)} \tag{33}$$

This must be equivalent to the experimental result, Equation (18)

$$b\epsilon^{H/H_1} \approx \frac{\Lambda_0 \omega}{C'(H, T)} \epsilon^{-\lambda(H, T)} \tag{34}$$

for $H \geq 5$ KOe. A convergent power-series expansion is next made for the exponent function, where the p's are taken in general to be T dependent:

$$\lambda(H, T) = p(T) + p_1(T) H + p_2(T) H^2 + \ldots$$

Intuitively it seems likely that $\lambda(H, T)$ has a slow monotonic dependence on H, so $\lambda(H, T)$ is assumed nearly linear. The justifiable procedure followed is to include higher-order terms in an improved approximation only if the fit to data necessitates it. Thus

$$\lambda(H, T) = p(T) + p_1(T) H \tag{35}$$

Substitution of Equation (35) into (34) yields the identifications

$$b(T) = \frac{\Lambda_o \bar{\omega}}{C'} \epsilon^{-p}, \quad \text{and } p_1 = -\frac{1}{H_1} \tag{36}$$

The b (T) identification implies field saturation of $\Lambda_o \bar{\omega}/C'$ has occurred for $H \geq 5$ KOe, $\epsilon \geq 0.26$.

The field-dependent exponent then is

$$\lambda = p - \frac{H}{H_1} = p + p_1 H \tag{37}$$

where experiment has shown that in the paramagnetic phase,

$$p = 1.56, \text{ and } p_1 = -\frac{1}{62.6} = -0.016 \text{ KOe}^{-1}$$

which are constants.

Recalling that $\lambda(H) = z - \alpha c$, where z is the critical index for the relaxation rate of order parameter fluctuations, and αc is the critical exponent for specific heat,[12] one suspects that the term $p_1 H$ may be describing αc, with the above value for p_1 in the paramagnetic phase. If for $H = 0$, $\alpha c = \alpha_o < 0$, a small negative constant,[1] (see Table I) then $\alpha c\,(H) = \alpha_o - p_1 H$, whence the specific heat follows the law

$$C_H \sim \epsilon^{\alpha c_o - p_1 H}$$

If this identification is possible, one sees that specific heat increases as H increases for $\alpha c_o < p_1 H$, and $\epsilon < 1$. Just this situation is seen for the isochamps of C_H for $CuK_2Cl_4 \cdot 2H_2O$ in the paper of Miedema, Van Kempen, and Huiskamp;[21] with $\epsilon > 0.1$. These isochamp intersections all occur within the near-critical isotherm range, $\epsilon \leq 0.1$. An assumption like $\alpha c_o = -0.02$ leads at least qualitatively to the behavior of C_H as described in the paper. It is hoped that the suggested form of the specific-heat index spurs further research into the matter.

4. Isotherms of the Non-Hydrodynamic Regime

If the regime index fulfills the condition $Z \ll 1$ (see the discussion of Equation (54) Chapter I), the Equation (31) becomes approximately

$$\Lambda \approx \Lambda_o (1 - Z),$$

representing the Kawasaki form for τ_M^{-1} in the non-hydrodynamic region.

The two near-critical isotherms, Figures 16 and 17, are too far from T_c to insure that the approximation is good. The case that $T = 0.96^o$ corresponds to $\epsilon = 0.09$, and $T = 0.815^o$ to $\epsilon = 0.08$, and these values of ϵ are near the boundary between the hydrodynamic and the non-hydrodynamic regimes.[18] (See the latter part of the discussion on ultrasonic attenuation, Chapter I).

The interpolation model described by Equation (31) and based on behavior in assymptotic limits, would be supported if it could be shown to fit these near-boundary isotherms. The similarity of the two isotherms, which brackett T_c, implies that the same function describes $T < T_c$ behavior as the $T > T_c$ behavior, for near-boundary isotherms. This condition is at least satisfied by the model.

One can solve Equation (31) for Z, getting

$$Z = \frac{\Lambda_o}{\Lambda} - 1 = \frac{\Omega'}{\bar{\omega}},$$

according to the model. One must know $\Lambda_o(H, T)$, which in turn necessitates knowledge of $a(T)$, and $H_o(T)$ (Equation (27)), in order to plot the function Z. If $\bar{\omega}$ is slowly changing with H, the plot then would reveal the behavior of Ω' with H. The graphic description would more accurately describe Ω' at high fields, where $\bar{\omega}$ saturates. This is said in the hope that further research will be initiated.

The data in this study is insufficient for proving validity of the model near the boundary of the critical region. More isotherms below 0.96°, and particularly below T_c are needed. Then, assuming the model, a computer program could be devised to reproduce the data, Λ, when correct trial functions $C'(H, T)$, and $\lambda(H, T)$ are substituted into Equation (31). These could possibly be series expansions of a few terms.

CHAPTER IV

SUMMARY

The interpolation formula

$$\tau_M^{-1} = \frac{D(H)\, x^2 T^3}{C(H)\epsilon^{\lambda(H)} + xT},$$

expressed equivalently by

$$\tau_M^{-1} = \frac{D'(H,T)\, \omega^2 T}{C'\epsilon^P + \omega},$$

where $C = \frac{\hbar}{k_B} C'$, $D = \frac{k_B}{\hbar} D' \tau_B$, and $x = \frac{\hbar\omega}{k_B T}$, has here been studied as a model for the magnetic scattering relaxation rate for phonon heat carriers in a crystal of $CuK_2Cl_4.2H_2O$. The symbols have the usual standard definitions.

Thermal conductivity data was used in a technique to get the thermal average $\langle \tau_M^{-1} \tau_D \rangle$ weighted by the thermal conductivity integrand. The results, expressed by plots at either constant field or constant temperature, are studied in terms of a two term formula derived in terms of the model. The field dependence of the parameters D', and $\lambda(H)$ are here summarized.

The coupling coefficient is expressed by

$$D'(H, T_c) = \sqrt{\frac{1.1}{1.1 + H}}, \text{ at } T_c = 0.88^{\circ},$$

the critical temperature. H is the field in KOe. The condition $\epsilon = \left|\frac{T}{T_c} - 1\right| \leq 0.1$ defines the critical region, where at high fields

$$D'(H, T) \sim (H_o(T) + H)^{-1/2}.$$

Here $H_o(T)$ is a phenomenological cutoff parameter; (thermal conductivity must be finite at H = 0). $H_o(T_c)$ = 1.1 KOe. The spin-interaction fields become a decreasing fraction of the ordering field, H, as H increases, so the interaction strength D' would be expected to decrease with an H increase.

The critical exponent for the magnetic rate of order-parameter fluctuations is found to be

$$\lambda(H) = p + p_1 H,$$

where p = 1.56 = $\lambda(0)$, according to previous results of Dixon, Rives, and Walton,[4] and p_1 = -0.016 KOc^{-1}, in the paramagnetic phase. Analysis of this was based on the linear semilog plots of isotherms in the hydrodynamic regime above 5 KOe.

It is suggested that the critical index for specific heat at constant H may be $\alpha = \alpha_o - p_1 H$, where α_o is a small negative constant. In the paramagnetic phase, this may explain why C_H increases with field for $\epsilon > 0.1$ as shown in the paper by Miedema, Van Kempen, and Huiskamp.[21] Low field isochamps of the thermal average $G = \langle \tau_M^{-1} \tau_D \rangle H$ behave like C_H, except that they do not cross.

Isotherms in the near-critical region have a structure not amenable to analysis in terms of the model, at the present state of knowledge. The interpolation model was selected on the basis of accuracy of description at two limiting conditions: $Z << 1$ (the non-hydrodynamic regime) and $Z >> 1$ (the hydrodynamic regime) where $Z = \Omega'/\bar{\omega}$ is the regime index. Ω' is the relaxation rate of order parameter fluctuations, and $\bar{\omega}$ an average frequency of the phonon distribution. Two isotherms of the critical region studied in this discussion

are near the boundary, $\epsilon = 0.09$, between the regimes; analysis based on the interpolation formula may be questionable. The formula may be indeed incorrect for them.

SELECTED BIBLIOGRAPHY

(1) Miedema, A. R., Wielinga, R. F., Huiskamp, W. J. Physica 31, 1585 (1965).

(2) Callaway, J. Phys. Rev. 113, 1046 (1959).

(3) Wood, D. W. and Dalton, N. W. Proc. Phys. Soc. 87, 755 (1966).

(4) Dixon, G. S., Rives, J. E., and Walton, D. "Critical Dynamics and Thermal Conductivities of Magnetic Insulators." July, 1970.

(5) Stanley, H. Eugene. "Introduction to Phase Transitions and Critical Phenomena." Oxford Press.

(6) Onsager, L. Phys. Rev. 65, 117 (1944).

(7) Pippard, A. B. Classical Thermodynamics. Cambridge: Cambridge University Press, 1961. p. 136 ff.

(8) Fairbanks, W. M., Buckingham, M. J., and Kellers, C. F. 1957 Proceedings of the Fifth International Conference on Low Temperature Physics. Madison, Wisconsin: University of Wisconsin Press.

(9) Orstein, L. S. and Zernicke, F. Proc. Sect. Sci. K. Med. Akad. Wet. 17, 793 (1914).

(10) Craig, P. P., and Goldburg, W. I. Jour. Appl. Physics, 40, 964 (1969).

(11) Halpern, B. S., and Hohenburg, P. C. Phys. Rev. 177, 952 (1969).

(12) Laramore, G., and Kadanoff, L. P. Phys. Rev., 187, 619 (1969).

(13) Kawasaki, K. J. Appl. Phys. 41, 1311 (1970).

(14) Stern, H. J. Phys. and Chem. Solids. 26, 153 (1965).

(15) Luthi, B., Moran, T. J., and Pollina, R. J. Phys. Chem. Solids 31, 1741 (1970).

(16) Kawasaki, K. Physics Letters, vol. 26A, 543 (1968).

(17) Dixon, G. S., Rives, J. E. and Walton, D. in "Dynamical Aspects of Critical Phenomena", Budwick and Kawatra, eds. Gordon and Breach, New York, 1972. p. 333.

(18) Haasbroek, J. N. Thermal Conductivity at very Low Temperatures (Thesis, Leiden, 1971).

(19) Roberts, T. R., Sherman, S. H., Sydoriak, S. G., and Brickwedde, F. G. Low Temperature Physics, vol. 4, C. J. Gorter, ed. New York: John Wiley, 1964. p. 480ff.

(20) Hetzler, M., and Walton, D. Rev. Sci. Instruc. 39, 1656 (1968).

(21) Miedema, A. R., Van Kempen, H., and Huiskamp, W. J. Physica 29, 1266 (1963).

(22) Dixon, G. S., and Johnson, R. W. "Field Dependence of Thermal Conductivity of $K_2CuCl_4 \cdot 2H_2O$ Near its Ferromagnetic Curie Temperature". Solid State Communications, vol. 13, pp. 1923-1925 (1973).

(23) Carruthers, P., Rev. Mod. Physics, vol. 33, No. 1, Jan. (1961).

(24) Herring, C. Phys. Rev. 95, 954 (1954).

(25) Peirels, R. Ann. Physik 3, 1055 (1929).

(26) Casimir, H. B. G. Physica 5, 495 (1938).

APPENDIX

A. Thermal Conductivity Theory

Knowledge of the theory of Thermal Conductivity in insulators is applicable to the extraction of information about critical phase transitions. A review of this theory is then appropriate.

1. The Heat Flux

Consider a system consisting of a crystal lattice and its energy. Under the assumption of small displacements, the hamiltonian operator for the system is

$$H = \sum_{\vec{k},\lambda} \hbar\omega_{\vec{k}\lambda} \left(\hat{N}_{\vec{k},\lambda} + \tfrac{1}{2}\right),$$

with eigenvalues $(n_{\vec{k},\lambda} + \tfrac{1}{2})\hbar\omega_{\vec{k},\lambda}$. Here, $n_{\vec{k},\lambda}$ is the number of phonons with wave vector $\vec{k}$, and polarization index λ.

The system is considered a Bose-gas of phonons having the equilibrium distribution

$$n^{o}_{\vec{k},\lambda} = \frac{1}{V\left(e^{\hbar\omega_{\vec{k},\lambda}/k_B T} - 1\right)} \tag{38}$$

where k_B is the Boltzmann constant, V is the system volume and T is the absolute temperature.

The phonon distribution is in general non-uniform throughout the system: local wave packets form from the normal modes; these conduct the heat through the system at group velocity

$$\vec{v}_{\vec{k},\lambda} = \nabla_k \omega_{\vec{k},\lambda} \qquad (39)$$

The heat flux through the system is

$$\vec{\dot{Q}} = \sum_{\vec{k},\lambda} n_{\vec{k},\lambda}(\vec{r}) h\omega_{\vec{k},\lambda} \vec{v}_{\vec{k},\lambda} \; ;$$

heat power per unit area conducted through the system, where $n_{\vec{k},\lambda}$ phonons/volume is the actual phonon distribution, unknown in the non-equilibrium case. One therefore makes use of small departures from equilibrium, $\delta n_{\vec{k},\lambda} = n_{\vec{k},\lambda} - n^{o}_{\vec{k},\lambda}$, an excess phonon density, in an approximation approach. For thermal equilibrium,

$$\vec{\dot{Q}}^{o} = \sum_{\vec{k},\lambda} n^{o}_{\vec{k},\lambda} \hbar\omega_{\vec{k},\lambda} \vec{v}_{\vec{k},\lambda} = 0$$

Then

$$\vec{\dot{Q}} - \vec{\dot{Q}}^{o} = \hbar \sum_{\vec{k},\lambda} \omega_{\vec{k},\lambda} \vec{v}_{\vec{k},\lambda} \delta n_{\vec{k},\lambda} = \vec{\dot{Q}}, \qquad (40)$$

the heat flux.

2. The Relaxation-Time Concept

Provided the departure of $n_{\vec{k},\lambda}$ from the equilibrium distribution is small, a good approximate expression for $\delta n_{\vec{k},\lambda}$ can be found. Since, through Liouville's Theorem

$$n(\vec{r} + \Delta\vec{r}, \vec{v} + \Delta\vec{v}, t + \Delta t) = n(\vec{r},\vec{v},t) + \Delta t \frac{\partial n}{\partial t} ,$$

one has $\nabla n.\vec{v} + \nabla_v n.\vec{\alpha} = \frac{\partial n}{\partial t}$, where $\vec{\alpha}$ is the acceleration of the gas of phonons. Subsequent experimental work is concerned only with the steady-state heat flow, however, for which $\vec{\alpha} = 0$. One then has the Boltzmann transport equation for phonon flow:

$$\frac{\partial n_{\vec{k},\lambda}}{\partial t} = \nabla n_{\vec{k},\lambda} \cdot \vec{v}_{\vec{k},\lambda} = \frac{\partial n_{\vec{k},\lambda}}{\partial T} \nabla T \cdot \vec{v}_{\vec{k},\lambda} ,$$

considering

$$n_{\vec{k},\lambda} = n_{\vec{k},\lambda}(T,t),$$

and using the chain rule.

Now the time dependence of $n_{\vec{k},\lambda}$ is due to diffusion via the temperature gradient, phonon scatter, and external fields. In this study, phonon scatter is due partly to low level states of paramagnetic ions in the material; external magnetic fields affect phonon scatter indirectly through these. There are also phonon collision processes intrinsic to the crystal being studied. The local time variations in $n_{\vec{k},\lambda}$ are due to phonon collisions, and a wave packet finds different temperature regions at correspondingly different times, as described by the Boltzmann equation

$$\frac{\partial n_{\vec{k},\lambda}}{\partial t}_{\text{collisions}} = \frac{\partial n_{\vec{k},\lambda}}{\partial T} \nabla T \cdot \vec{v}_{\vec{k},\lambda} \qquad (41)$$

If the heat processes are suddenly removed, scattering processes act to restore equilibrium, which is theoretically never reached. There is a characteristic time $\tau_{\vec{k},\lambda}$, to be called a relaxation time, associated with the approach. For the $\vec{k},\lambda$ set of phonons, it is defined by

$$\frac{1}{\tau_{\vec{k},\lambda}} \int_{\tau_{\vec{k},\lambda}}^{0} \frac{\partial n_{\vec{k},\lambda}}{\partial t} \, dt = - \frac{\partial n_{\vec{k},\lambda}}{\partial t}\Big|_{\text{Ave}} = \frac{\delta n_{\vec{k},\lambda}}{\tau_{\vec{k},\lambda}}$$

If $\tau_{\vec{k},\lambda}$ is small the average derivative differs negligibly from the integrand, and one has

$$\frac{\partial n_{\vec{k},\lambda}}{\partial t} = -\frac{\delta n_{\vec{k},\lambda}}{\tau_{\vec{k},\lambda}} \tag{42}$$

Considering only time-dependence, the solution of this equation is

$$n_{\vec{k},\lambda} = n^{o}_{\vec{k},\lambda} e^{-t/\tau_{\vec{k},\lambda}}$$

showing $\tau_{\vec{k},\lambda}$ to be a characteristic time for exponential decay of $\delta n_{\vec{k},\lambda}$ to equilibrium: $\delta n_{\vec{k},\lambda} = 0$.

For the slight departure from equilibrium, the approximation

$$\frac{\partial n_{\vec{k},\lambda}}{\partial T} \approx \frac{\partial n^{o}_{\vec{k},\lambda}}{\partial T} \tag{43}$$

is also valid.

Solving Equation (42) for $\delta n_{\vec{k},\lambda}$, substituting from Equation (41) and then from Equation (43), one gets

$$\delta n_{\vec{k},\lambda} \approx -\tau_{\vec{k},\lambda} \frac{\partial n^{o}_{\vec{k},\lambda}}{\partial T} \nabla T \cdot \vec{v}_{\vec{k},\lambda} \tag{44}$$

This, in turn, substituted into Equation (40), yields the heat-flow equation

$$\vec{\dot{Q}} = -\hbar \sum_{\vec{k},\lambda} \tau_{\vec{k},\lambda} \omega_{\vec{k},\lambda} \frac{\partial n^{o}_{\vec{k},\lambda}}{\partial T} \vec{v}_{\vec{k},\lambda} \vec{v}_{\vec{k},\lambda} \cdot \nabla T \tag{45}$$

in which relaxation times explicitly appear.

3. The Debye Theory of Thermal Conductivity

Now

$$\hbar \omega_{\vec{k},\lambda} \frac{\partial n^{o}_{\vec{k},\lambda}}{\partial T} = C_{\vec{k},\lambda} \tag{46}$$

is the contribution to the specific heat at constant volume for the k mode, λ^{th} polarization component. Then the dyadic

$$\bar{\bar{K}} = \sum_{\vec{k},\lambda} \tau_{\vec{k},\lambda} C_{\vec{k},\lambda} \vec{v}_{\vec{k},\lambda} \vec{v}_{\vec{k},\lambda}$$

is a thermal conductivity tensor, in terms of wnich the heat conduction vector (45) is

$$\vec{Q} = - \bar{\bar{K}} \cdot \nabla T.$$

The subsequent investigation is concerned only with heat conduction in the direction of the temperature gradient. Let the ∇T direction be that of the z axis. $\theta_{\vec{k},\lambda}$ is to be the direction of $\vec{v}_{\vec{k},\lambda}$ with respect to this axis. The thermal conductivity in this direction is

$$K = \sum_{\vec{k},\lambda} \tau_{\vec{k},\lambda} C_{\vec{k},\lambda} v^2_{\vec{k},\lambda} \cos^2 \theta_{\vec{k},\lambda} \qquad (47)$$

One now approximates this discrete state distribution by a continuous distribution in k-space. The summation may be approximated then by an integral as follows:

The normal modes are travelling waves, governed by the periodic boundary conditions $L_1 = N_{\vec{k}1\vec{k}}$ (L_1 is one dimension of the solid, considered a rectangular parallelopiped); similarly, $L_2 = N_{\vec{k}2} \lambda_{\vec{k}2}$, $L_3 = N_{\vec{k}3} \lambda_{\vec{k}3}$; $\lambda_{\vec{k}i}$ are wavelengths; $N_{\vec{k}i}$ are integers. Then $\lambda_{\vec{k}i} = L_i / N_{\vec{k}i}$, whence $k_i = 2\pi/\lambda_i = (2\pi/L_i) N_{\vec{k}i}$. One has $\Delta k_1 \Delta k_2 \Delta k_3 = \Delta^3 V_k = (2\pi)^3 / V \Delta N_1 \Delta N_2 \Delta N_3$, the permissable volume increments in k-space. The smallest non vanishing volume-increment results when $\Delta N_1 = 1 = \Delta N_2 = \Delta N_3$, i.e., $V/(2\pi)^3 \, d^3 V_k = 1$, where $V = L_1 L_2 L_3$, the solid volume. Multiplying each term in the above summation (47) by unity doesn't change the

summation, so

$$K = \frac{V}{(2\pi)^3}\sum_{\lambda}\int_{0}^{V_{k\,max}} \tau_{\vec{k}\lambda}\, C_{\vec{k}\lambda}\, v^2_{\vec{k}\lambda}\, \cos^2\theta_{\vec{k}\lambda}\, d^3V_{\vec{k}\lambda}.$$

It is convenient to treat the approximate differential in polar spherical coordinates

$$d^3V_k = k^2 dk \sin\theta d\theta d\phi,$$

whence

$$K = \frac{V}{(2\pi)^3}\sum_{\lambda}\int_{0}^{V_{k\,max}} \tau_{\vec{k},\lambda}\, C_{\vec{k},\lambda}\, v^2_{\vec{k},\lambda}\, \cos^2\theta_{\vec{k},\lambda}\, (-d\cos\theta_{\vec{k},\lambda})\, d\phi k^2 dk.$$

The angle integrations carried out, one has the integral over the first Brillouin Zone

$$K = \frac{V}{(2\pi)^2}\,\frac{2}{3}\sum_{\lambda}\int_{0}^{k_{max}} \tau_{\vec{k},\lambda}\, C_{\vec{k},\lambda}\, v^2_{\vec{k},\lambda}\, k^2\, dk,$$

which is the general expression for thermal conductivity.

There are three polarization directions; the integral is the same for each component, so finally

$$K = \frac{V}{2\pi^2}\int_{0}^{k_{max}} \tau_{\vec{k}}\, C_{\vec{k}}\, v^2_{\vec{k}}\, k^2\, dk \qquad (48)$$

The crude thermal conductivity of elementary kinetic theory is readily found from this through the mean value theorem of integrals. Thus,

$$K = \frac{V}{2\pi^2}\,\langle Cv\,(v\tau)\rangle\int_{0}^{k_{max}} k^2 dk = \text{const. x } C\bar{v}\Lambda,$$

where Λ is the average phonon mean-free path, and $\bar{v}$ is the average phonon velocity.

Evaluation of the integral in (48) involves the acoustic approximation $\omega_{\vec{k}} = v_{\vec{k}}\, k$. If this is not involved, or $\omega_{\vec{k}}$ depends on T, one must use the integral (48) in its general form. In the subsequent work, the acoustic approximation is assumed, which leads to the Debye equation for thermal conductivity of an isotropic solid. Substituting (46) into (48), one gets

$$K = \frac{\hbar v}{2\pi^2} \int_0^{k_{max}} \tau_k \omega_k \frac{\partial n^o_k}{\partial T} v^2_k k^2 \, dk, \text{ where,} \tag{49}$$

using (38)

$$\frac{\partial n^o_k}{\partial T} = \frac{\frac{\hbar \omega_k}{k_B T^2} e^{\frac{\hbar \omega_k}{k_B T}}}{\left(\frac{\hbar \omega_k}{k_B T} - 1\right)^2 v}, \text{and } k = \frac{\omega_k}{v} \tag{50}$$

For isotropic media, $v_k = v$ is the acoustic velocity, assumed the same for all modes of vibration, and taken to be constant. Thus, also, $dk = d\omega_k / v$. Substituting (50) into (49), one gets

$$K = \frac{\hbar v}{2\pi^2 v} \int_0^{\omega_{max}} \tau(\omega) \omega \frac{\hbar \omega}{k_B T^2} \frac{e^{\hbar \omega / k_B T}}{\left(e^{\hbar \omega / k_B T} - 1\right)^2} \omega^2 d\omega.$$

One defines the dimensionless variable

$$X = \frac{\hbar \omega}{k_B T}$$

whence

$$\omega^2 d\omega = \left(\frac{k_B T}{\hbar}\right)^3 x^2 \, dx,$$

and

$$K = \left(\frac{k_B T}{\hbar}\right)^3 \frac{k_B}{2\pi^2 v} \int_0^{\Theta/T} \tau(\omega) X^2 \frac{e^x}{(e^x - 1)^2} X^2 \, dx,$$

or finally the Debye expression for thermal conductivity is

$$K = \frac{k_B^4 T^3}{2\pi^2 \hbar^3 v} \int_0^{\Theta/T} \tau(x) \frac{x^4 e^x}{(e^x - 1)^2} \, dx, \qquad (51)$$

where $\Theta = \hbar \omega_{max}/k_B$ is the Debye temperature.

B. Relaxation-Time Rationale

1. Law of Combination of Relaxation Times

Attention now focuses on $\tau(x)$, hereafter called the combined relaxation time, or the lifetime for nonequilibrium states, labelled $\hbar\omega$, to decay to the equilibrium states.

There are many different phonon scattering processes; one properly adds their respective scattering amplitudes (i.e., the wave functions) and computes net scattering probability from this sum. However, if tne scattering centers are sufficiently separated, the scattering is mostly incoherent, which permits addition of cross-sections, each numerically an independent probability for a collision process, to get total scattering probability. Thus, if the cross section for the k^{th} moade in process i is $_{ki}$, the mean free path is

$$\Lambda_{ki} = \frac{1}{n \sigma_{ki}} = \tau_i v_k .$$

whence

$$\sigma_{ki} = \frac{1}{n v_k \tau_i} = \frac{1}{n \Lambda_{ki}} .$$

The number of scattering centers per unti volume is n. The scattering probability for all the different processes is then $\sigma_k = \sum_i \sigma_{ki} = 1/n\, v_k \sum_i 1/\tau_i = 1/n\, v_k \tau$; τ_i are the scattering relaxation times

for the different processes.

Thus, $\frac{1}{\tau} = \sum_i \frac{1}{\tau_i}$ is assumed, valid only if scattering probabilities are independent. Validity has been examined theoretically and experimentally, it seems that for low temperatures the effects of different scattering processes are properly combined thus.

2. Relaxation Times for Different Scattering Processes

There remains a discussion of the scattering mechanisms, and their relaxation times. There are phonon-phonon interactions, point defect, boundary, and magnetic ordering interactions with phonons. These are here considered with their regions of dominant contribution to the thermal conductivity.

a. Phonon-Phonon Interactions

Only three-phonon interactions are considered; mutual interactions among more than three are believed of very low probability. The three-phonon interaction gives rise to either of two processes; normal processes, and umklapp processes.

Normal processes are described by conservation of energy, $\hbar\omega_1 + \hbar\omega_2 = \hbar\omega_3$, and conservation of momentum, $\vec{k}_1 + \vec{k}_2 = \vec{k}_3$; these give no contribution to thermal resistance, their effect is indirect, through stabilizing the equilibrium distribution.

Umklapp processes, for which momentum is not conserved, are described by

$$\vec{k}_1 + \vec{k}_2 = \vec{k}_3 + \vec{G};$$

$\vec{k}_1 + \vec{k}_2$ is outside the first Brillouin Zone; $\vec{G}$ is that reciprocal

lattice vector necessary to return $\vec{k_3}$ to the first Brillouin Zone. The effect, equivalent to a Bragg reflection of crystal planes, means that some total momenta each have a component that is reversed in direction from the corresponding component of the vector sum $\vec{k_1} + \vec{k_2}$, hence the term "Umklapp Scattering."

A short plausibility treatment of relaxation time for umklapp processes is introduced for the sake of continuity, based on the integral theorem of the mean value. Umklapp processes begin for two interacting phonons which have each reached a momentum corresponding to a wave vector $\vec{k}$ which equals half the effective radius of a Brillouin Zone.[23] Call this wave vector $\vec{k}_{min}$, and consider that only umklapp processes are occurring, or equivalently, that these processes are dominant. The thermal conductivity for these processes is

$$K_U(T) = AT^3 \int_{x\ min}^{\Theta/T} \tau_U(X)\, e^{-x} \left(\frac{X^2}{1 - e^{-x}}\right)^2 X^2\, dx$$

According to the theorem, there is some X', $X_{min} < X' < X_{max}$, for which

$$K_U(T) = AT^3\, \tau_U(X') X'^2\, e^{-X'} \int_{X_{min}}^{X_{max}} \left(\frac{X}{1 - e^{-x}}\right)^2 dX.$$

The value X' corresponds to a particular wave-vector, say k' = q. At a given temperature,

$$\tau_U(X') \sim \frac{K_U}{T^3\, e^{-X'}\, X'^2},$$

where

$$X' = \frac{\hbar\,\omega(q)}{k_B T} = \frac{\Theta}{\omega_{max}} \frac{\omega(q)}{T} = \Theta/\alpha T,$$

and $= \omega_{max}/\omega(q)$ is a constant, fitted by experiment. The expression for τ_U is of the form usually used; X' is proportional to $\omega(q)$: one assumes Herring's relaxation time for phonon-phonon scattering, $\omega^2 T^3$, and

$$\tau_U(X') = \frac{1}{bT^3 e^{-\Theta/\alpha T} \omega^2} \tag{52}$$

where b is a constant.[24] Of course, the dummy variable X' becomes X in applications, but α remains constant. The thermal resistance, K_U^{-1}, is proportional to T at high temperatures, and falls exponentially at low temperatures, as Peierls discovered.[25] Umklapp processes are important typically for $\Theta/T < 20$; are of consequences above the temperature of maximum K, unimportant below it. As the K peak is near 10 K in $CuK_2Cl_4 \cdot 2H_2O$, these processes are unimportant.

b. Point Defect Scattering

Point defects, such as vacancies, interstitials, impurity ions, and isotope ions, produce diffraction scatter according to the Rayleigh scattering formula borrowed from optics. For the isotope ion, the scatter probability is

$$\sigma(k) = \frac{k^4}{4\pi D^2} (\delta M)^2,$$

where δM is the point mass, D is the crystal density. Thus,

$$\sigma(k) \sim \omega^4,$$

and

$$\tau_p = \frac{1}{A' \omega^4}$$

is the point defect relaxation time, which also can be expressed

$$\tau_p = \frac{1}{Bx^4T^4} ; \qquad (53)$$

A' and B are constants fitted by experiment. Thermal conductivity due to point defects is greatest for low frequencies; thermal resistance increases fast with frequency, as point defects begin to dominate. As point defect scatter is appreciable before the k_{min} of the umklapp processes is reached, this relaxation time is included in the combined relaxation time, τ.

c. Boundary Scattering

Boundary scattering of phonons affects conductivity in the following way. The mean-free path, Λ_k^o, for scattering, is inversely proportional to the number-density of scattering centers. Λ_k^o is dominated by phonon-phonon processes at high temperatures; as temperature falls, the number density of phonons present lowers, and the mean-free path increases. These are long wavelength phonons for which $\Lambda_{ki}^o \geq L$, a crystal dimension. For these, Λ_{ki}^o can't increase. As temperature lowers, eventually thermal resistivity is dominated by such phonons. The crude thermal conductivity expression $K \approx$ const. x $c_v v \Lambda$ suffices to show, that as $\Lambda \approx L$, K must decrease with further temperature decrease because this is the behavior of the mean specific heat, c_v. K reduces to a T^3 law near 0 K.

Casimir[26] likened a long crystal to a cylindrical tube with perfectly black walls, and the phonon gas to a photon gas. To this he applied block-body radiation theory, with T low enough that phonon-phonon interactions were negligible, the walls were such that radiation

was diffusely scattered.

The result was a boundary-scatter relaxation time

$$\tau_B = \frac{L}{v} ,$$

where L is a Casimir length[26] computed from the crystal geometry. For a square cross-section, of side a, L = 1.12 a. For a rectangular cross section, say .3 cm x .5 cm, L = .4 cm. More generally, L = 1.12 A, A being the sample cross-section.

d. Scattering Due to Magnetic Ordering

The magnetic-order scattering relaxation time is here introduced, which is to be the object of investigation. It is postulated[4] to fit the Laramore and Kadonoff[12] Theory, and the Kawasaki[13] conditions:

$$T_M^{-1} = \frac{D'\omega^2 T}{C'|\epsilon|^p + \omega} , \qquad (54)$$

where

$$\epsilon = \frac{T - T_c}{T_c} ,$$

and T_c is the Curie-point for the magnetic phase transition, p is a critical exponent, and D', C' are constants.

C. The Use of Thermal Conductivity

The reciprocal lifetime of the scattering processes within the temperature range of investigation is then

$$\frac{1}{\tau} = \frac{1}{\tau_B} + \frac{1}{\tau_P} + \frac{1}{\tau_M} = \frac{v}{L} + A'\omega^4 + \frac{D'T\omega^2}{C'|\epsilon|^p + \omega}$$

It is convenient to define

$$C = \frac{\hbar}{k_B} C' , \text{ and } D = \frac{k_B}{\hbar} \tau_B D' , \text{ whence}$$

$$\tau = \frac{L}{v} \quad \frac{1}{1 + BT^4X^4 + \frac{DX^2T^3}{C|\epsilon|^p + TX}} \tag{55}$$

expresses the lifetime in terms of the parameter X. The denominator terms are dimensionless forms of relaxation-rates:

$$\tau_D^{-1} = 1 + BT^4X^4;$$

the "diamagnetic" rate or boundary and point-defect rates combined, and

$$\tau_M^{-1} = \frac{DX^2 T^3}{\Omega + TX}, \tag{56}$$

the assumed magnetic scattering relaxation rate. $\Omega = C\epsilon^p$ is the rate of magnetic ordering fluctuations, corresponding to $\Omega' = C'\epsilon^p$.

The thermal conductivity, where A, C, and D are constants, is then

$$K = AT^3 \int_0^{H_K} \frac{X^4 e^x dx}{(e^x - 1)^2 \left(1 + BT^4X^4 + \frac{DT^3X^2}{C\epsilon^p + TX}\right)}, \tag{57}$$

which is the analytical tool for exploring the magnetic phase transition phenomena near the critical temperature, T_c. The constant A is

$$A = \frac{k_B^4 V T^3 L}{2\pi^2 \hbar^3 v^2},$$

and constants, B, C, D, and p are fitted by experiment.

VITA

Robert Wendell Johnson

Candidate for the Degree of

Doctor of Philosophy

Thesis: THERMAL CONDUCTIVITY OF $CuK_2Cl_4 \cdot 2H_2O$ IN APPLIED MAGNETIC FIELDS NEAR ITS CURIE POINT

Major Field: Physics

Biographical:

Personal Data: Born in Fowler, Kansas, July 21, 1922, the youngest child of James Hans and Cordelia Rachel Johnson. Married Karen Constance Holmgren on February 21, 1959.

Education: Finished grade school in Meade, Kansas, High School in North Kansas City, Missouri. Received a Bachelor of Science degree in Electrical Engineering, 1948; and a Master of Science degree in Physics, 1952, from the University of Kansas. Completed requirements for the Doctor of Philosophy degree at Oklahoma State University in July, 1974.

Professional Experience: Research Engineer, Midwest Research Institute, Kansas City, Missouri, 1951, 1952. Engineer, Boeing Airplane Company, Wichita, Kansas, 1952-1960. Assistant Professor of Physics, Friends University, Wichita, Kansas, 1960-1970. Teaching Assistant, Oklahoma State University, Stillwater, Oklahoma, 1957-1958, and Fall and Spring of 1970-1971, and also of 1971-1972. Research Assistantship at Oklahoma State University in Summer of 1971. Member of Sigma Pi Sigma, Oklahoma State University and of Sigma Xi.